Cell Reports

Resource

PP2A$_C$ Phospho-Tyr^{307} Antibodies Are Not Specific for this Modification but Are Sensitive to Other PP2A$_C$ Modifications Including Leu^{309} Methylation

Graphical Abstract

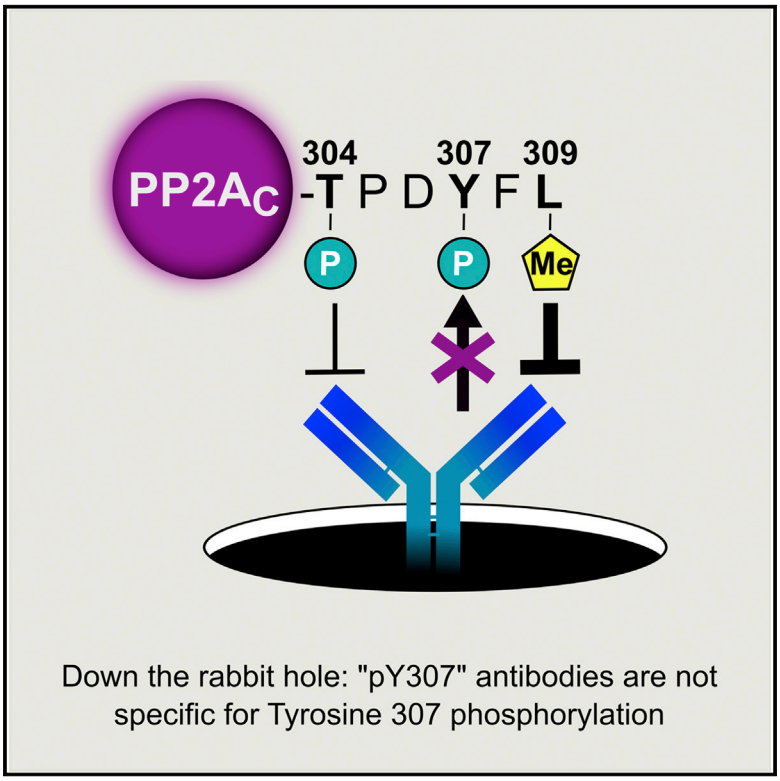

Down the rabbit hole: "pY307" antibodies are not specific for Tyrosine 307 phosphorylation

Highlights

- PP2A$_C$ phospho-Tyr^{307} antibodies are not specific for this modification
- All are sensitive to PP2A$_C$ Leu^{309} methylation, some to Thr^{304} phosphorylation
- Some cross-react with pTyr residues in general, including phosphorylated HA tags
- Publications claiming PP2A inhibition using pTyr307 antibodies need reinvestigation

Authors

Ingrid E. Frohner, Ingrid Mudrak, Stefan Schüchner, ..., Teresa Preglej, Wilfried Ellmeier, Egon Ogris

Correspondence

egon.ogris@meduniwien.ac.at

In Brief

Tyrosine phosphorylation of PP2A catalytic subunit (Tyr^{307}) is presumed to inhibit its activity. Frohner et al. report that antibodies used to study this modification are not specific for the targeted phospho-site but instead are impaired by modifications of nearby sites, suggesting a mechanism of PP2A inhibition different than proposed previously.

Frohner et al., 2020, Cell Reports *30*, 3171–3182
March 3, 2020
https://doi.org/10.1016/j.celrep.2020.02.035

CellPress

Cell Reports
Resource

$PP2A_C$ Phospho-Tyr^{307} Antibodies Are Not Specific for this Modification but Are Sensitive to Other $PP2A_C$ Modifications Including Leu^{309} Methylation

Ingrid E. Frohner,[1] Ingrid Mudrak,[1] Stefan Schüchner,[1] Dorothea Anrather,[2] Markus Hartl,[2] Jean-Marie Sontag,[3] Estelle Sontag,[3] Brian E. Wadzinski,[4] Teresa Preglej,[5] Wilfried Ellmeier,[5] and Egon Ogris[1,6,*]

[1]Center for Medical Biochemistry, Max Perutz Labs, Medical University of Vienna, Dr. Bohr-Gasse 9, 1030 Vienna, Austria
[2]Mass Spectrometry Facility, Max Perutz Labs, Dr. Bohr-Gasse 9, 1030 Vienna, Austria
[3]School of Biomedical Sciences and Pharmacy, The University of Newcastle, Callaghan, NSW 2308, Australia
[4]Department of Pharmacology, Vanderbilt University School of Medicine, Nashville, TN 37232, USA
[5]Division of Immunobiology, Institute of Immunology, Center for Pathophysiology, Infectiology and Immunology, Medical University of Vienna, 1090 Vienna, Austria
[6]Lead Contact
*Correspondence: egon.ogris@meduniwien.ac.at
https://doi.org/10.1016/j.celrep.2020.02.035

SUMMARY

Protein phosphatase 2A (PP2A) is an important regulator of signal transduction pathways and a tumor suppressor. Phosphorylation of the PP2A catalytic subunit ($PP2A_C$) at tyrosine 307 has been claimed to inactivate PP2A and was examined in more than 180 studies using commercial antibodies, but this modification was never identified using mass spectrometry. Here we show that the most cited $pTyr^{307}$ monoclonal antibodies, E155 and F-8, are not specific for phosphorylated Tyr^{307} but instead are hampered by $PP2A_C$ methylation at leucine 309 or phosphorylation at threonine 304. Other $pTyr^{307}$ antibodies are sensitive to $PP2A_C$ methylation as well, and some cross-react with pTyr residues in general, including phosphorylated hemagglutinin tags. We identify $pTyr^{307}$ using targeted mass spectrometry after transient overexpression of $PP2A_C$ and Src kinase. Yet under such conditions, none of the tested antibodies show exclusive $pTyr^{307}$ specificity. Thus, data generated using these antibodies need to be revisited, and the mechanism of PP2A inactivation needs to be redefined.

INTRODUCTION

Protein phosphatase 2A (PP2A), a phospho-serine/threonine-directed phosphatase, plays a crucial role in the control of cell growth and proliferation. Deregulation or inactivation of PP2A is implicated in a variety of diseases, such as cancer and Alzheimer's disease (AD) (Narla et al., 2018; Sontag and Sontag, 2014). The PP2A holoenzyme is a heterotrimer containing three subunits, a catalytic C subunit ($PP2A_C$), a scaffolding A subunit, and one of multiple regulatory B-type subunits (Virshup and Shenolikar, 2009). PP2A heterotrimer assembly and activity are tightly controlled by multiple regulatory mechanisms, including post-translational modifications (Sents et al., 2013).

A key regulatory event in the assembly of the heterotrimer is carboxymethylation of leucine 309 (Leu^{309}) within the highly conserved C-terminal $PP2A_C$ sequence $TPDYFL^{309}$. In addition, this sequence has been reported to be phosphorylated on tyrosine 307 (Tyr^{307}) and threonine 304 (Thr^{304}) (Chen et al., 1992; Ogris et al., 1997; Schmitz et al., 2010). C-terminal methylation is essential for the maturation of active PP2A holoenzymes (Fellner et al., 2003; Ogris et al., 1997; Stanevich et al., 2011; Tolstykh et al., 2000; Yu et al., 2001), while phosphorylation of $PP2A_C$ subunit (on either Tyr^{307} or an undefined threonine residue) has been primarily associated with the inhibition of its catalytic activity (Chen et al., 1992, 1994; Damuni et al., 1994; Guo and Damuni, 1993). However, inhibition of PP2A catalytic activity by recombinant Src-mediated Tyr^{307} phosphorylation could only be shown with thiophosphorylated purified $PP2A_C$ subunit, because the putative inhibitory phosphate was apparently rapidly removed via an autocatalytic reaction. Importantly, only indirect experimental evidence exists for phosphorylation at Tyr^{307} *in vivo* (Chen et al., 1992), which raises concerns about the physiological role and importance of this site.

Inhibition of PP2A and its tumor-suppressive function by Tyr^{307} phosphorylation has represented an attractive hypothesis in the cancer field. Since the first report in 1992 (Chen et al., 1992), more than 180 studies have used commercial antibodies to describe regulated as well as pathologic changes in PP2A Tyr^{307} phosphorylation levels in a variety of cell types (Brautigan, 2013). However, essentially all of these studies have relied on poorly validated commercial $PP2A_C$ $pTyr^{307}$ antibodies for the detection of this modification (see "Mendeley: list of publications using commercial $PP2A_C$ $pTyr^{307}$ antibodies"). The most frequently cited antibody for the detection of $pTyr^{307}$ is a rabbit monoclonal antibody, clone E155, generated by Epitomics (1155-1, Abcam). Clone E155 was used for the detection of $pTyr^{307}$ PP2A in 112 publications between 2005 and 2019. In 2016, on the basis of a customer's concern about the antibody's specificity, Abcam re-examined the antibody and clarified that it was not specific for $pTyr^{307}$. Since then the antibody has been

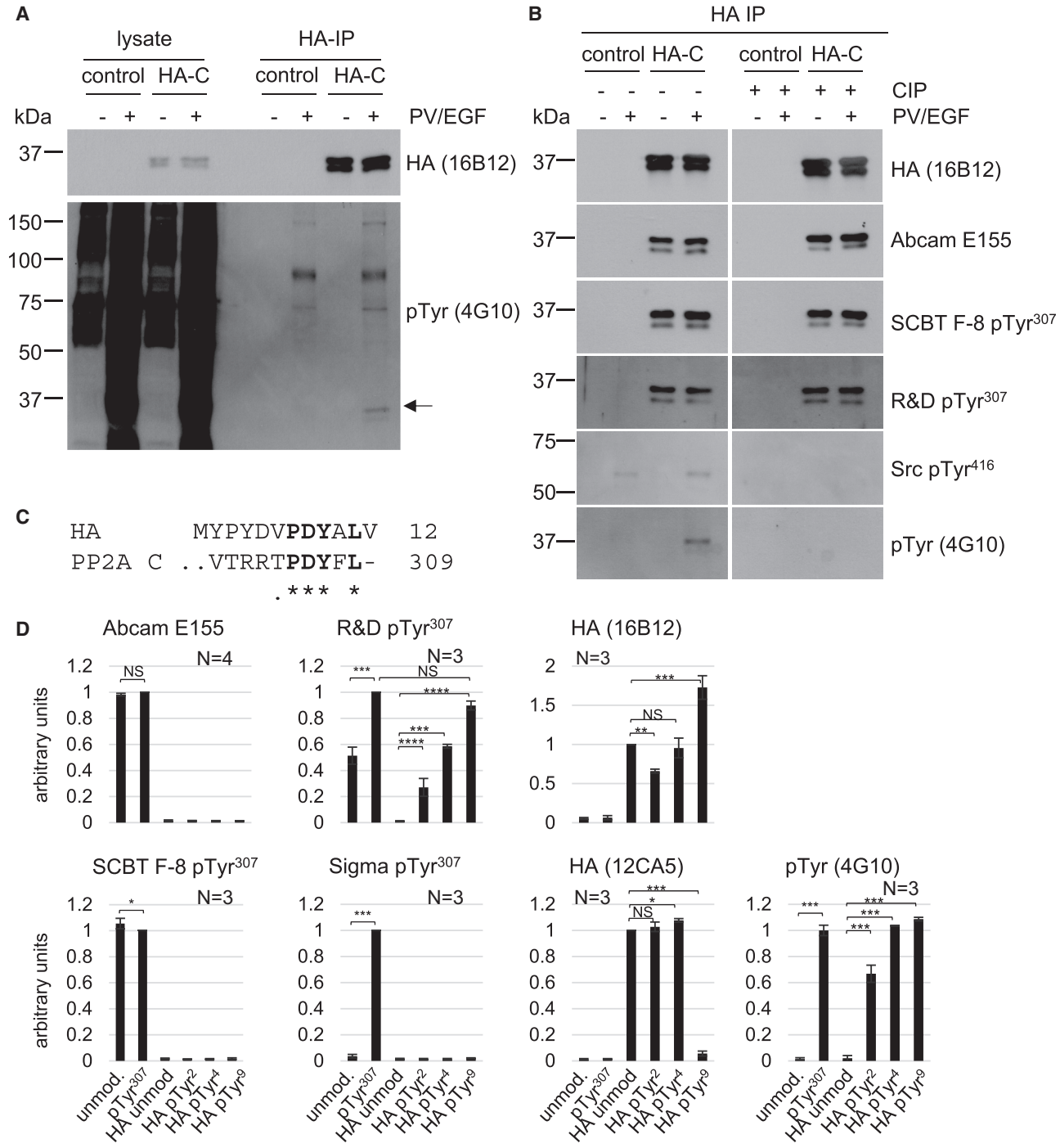

Figure 1. "PP2A$_C$ pTyr^{307}" Antibody Signals Are Not Increased upon Stimulation of NIH 3T3 Cells with EGF and Pervanadate

(A) Immunoblotting of lysates and HA-immunoprecipitates of NIH 3T3 cells infected with either pBabe puro (control) or pBabe puro HA-PP2A$_C$ subunit (HA-C) using the indicated antibodies. Cells were starved with 0.5% fetal bovine serum (FBS) and either left untreated (–) or pervanadate/EGF treated (+). The panel originates from 2 blotting membranes.

(B) Immunoblotting of HA-immunoprecipitates of (A) with the indicated antibodies. Phosphate groups on proteins were removed by CIP treatment (right panels). The panels originate from 12 different blotting membranes. The blots are representative of two independent experiments.

(C) Alignment of the PP2A$_C$ C terminus and the HA epitope tag sequence.

(D) Quantification of binding of the indicated antibodies to peptides unmod (HVTRRTPDYFL), pTyr^{307} (HVTRRTPDpYFL), HA unmod (MYPYDVPDYALV), HA pTyr^2 (MpYPYDVPDYALV), HA pTyr^4 (MYPpYDVPDYALV), or HA pTyr^9 (MYPYDVPDpYALV). Antibody binding data are shown as the average and standard

(legend continued on next page)

remarketed as a general PP2A antibody for the detection of the alpha and beta isoforms of the catalytic C subunit. Despite the relabeling, this antibody has continually been used for the detection of pTyr^{307} in at least 26 studies since 2017. We were also puzzled by the fact that E155, a supposedly general PP2A antibody, detected fluctuating PP2A expression levels in many of these studies, whereas control antibodies showed stable PP2A$_C$ levels (Du et al., 2015, 2018; Dudiki et al., 2015; Gu et al., 2015; Huang et al., 2017; Kim et al., 2008; Liu et al., 2016; Mukhopadhyay et al., 2017; Sun et al., 2014; Wang et al., 2013, 2014, 2017; Xu et al., 2016). Consequently, we postulated that features distinct from Tyr^{307} phosphorylation must exist for the observed fluctuation in detection levels (Ogris et al., 2018).

In addition to E155, there are several other frequently cited commercial "PP2A$_C$ pTyr^{307}" antibodies, which include mouse monoclonal F-8 (sc-271903), goat polyclonal (sc-12615, discontinued), and rabbit polyclonal (sc-12615-R, discontinued) from Santa Cruz Biotechnology (SCBT), R&D Systems rabbit polyclonal (AF3989), mouse monoclonal 4B10 (Millipore 05-547, discontinued, also available from BioLegend/Covance, BioTechne/Novus, and SCBT), Sigma-Aldrich rabbit polyclonal (SAB4503975), and Thermo Fisher Scientific rabbit polyclonal (PA5-36874). In the present study, we thoroughly tested these commercial "PP2A$_C$ pTyr^{307}" antibodies for their target specificity, off-target properties, and potential cross-reactivities. We found that the most frequently cited pTyr^{307} monoclonal antibodies, E155 and F-8, were unable to discriminate between Tyr^{307} and pTyr^{307} but were instead sensitive to PP2A$_C$ Leu^{309} methylation. None of the tested antibodies possessed absolute specificity for pTyr^{307}, and their binding was influenced by concurrent phosphorylation of Thr^{304} and/or methylation of Leu^{309}. Remarkably, some of the widely used antibodies even cross-reacted with the HA epitope tag that can be tyrosine-phosphorylated in cells. We conclude that all prior studies based on commercial "PP2A$_C$ pTyr^{307}" antibodies should be carefully re-evaluated.

RESULTS

PP2A$_C$ pTyr^{307} Antibodies Do Not Show an Increased Signal upon Induction of PP2A$_C$ Tyrosine Phosphorylation

Transformation of mammalian cells with p60$^{v\text{-}Src}$, as well as stimulation of quiescent cells with EGF, has been reported to result in tyrosine phosphorylation of PP2A$_C$ (Chen et al., 1994). To test whether commercial mono- and polyclonal pTyr^{307} antibodies are able to detect Tyr^{307}-phosphorylated PP2A, we first expressed N-terminal HA-tagged PP2A$_C$ in NIH 3T3 cells and then serum-starved the cells overnight prior to treatment for 15 min with EGF and pervanadate (PV) (Huyer et al., 1997). As expected, western analyses of total cell lysates with anti-pTyr 4G10 antibody revealed that stimulation with EGF/PV significantly enhanced endogenous protein tyrosine phosphorylation relative to untreated cells. A weak signal corresponding to tyrosine-phosphorylated HA-PP2A$_C$ was also observed in immunoprecipitates prepared from total homogenates of EGF- and PV-stimulated cells (Figure 1A). Notably, immunoreactivity with 4G10 antibody could be completely removed by treatment with calf intestinal phosphatase (CIP), thereby confirming that the observed signals were indeed due to tyrosine phosphorylation (Figure 1B). In contrast to what was observed with generic 4G10 pTyr antibody, HA-PP2A$_C$ immunoprecipitated from starved untreated cells was strikingly immunoreactive to all tested monoclonal (E155, F-8) and rabbit polyclonal PP2A$_C$ pTyr^{307} antibodies (from R&D Systems and SCBT). Moreover, immunoreactivity did not increase upon stimulation of cells with EGF/PV and was insensitive to CIP treatment in these cells (Figure 1B; Figure S1A). Similar results were obtained with the E155 antibody in PV-treated Cos-7 and N2a cell lysates (Figures S1D and S1E). A goat polyclonal PP2A$_C$ pTyr^{307} antibody (SCBT) and monoclonal 4B10 antibody (from our laboratory) that detect pTyr^{307} in ELISAs failed to recognize HA-PP2A$_C$ immunoprecipitated from either untreated or treated cells (Figure S1A).

Given the lack of specificity of the PP2A$_C$ Tyr^{307} antibodies, we asked whether HA-PP2Ac is indeed phosphorylated on Tyr^{307} by comparatively analyzing using mass spectrometry (MS) the HA-PP2A$_C$ immune complexes prepared from untreated and EGF/PV-treated NIH 3T3 cells. A global untargeted phosphopeptide analysis failed to detect Tyr^{307} phosphorylation but identified known PP2A$_C$ phosphorylation sites (Gu et al., 2011; Kettenbach et al., 2011; Luo et al., 2008) and, surprisingly, phosphorylation of Tyr^4 of the HA epitope tag in EGF/PV-treated NIH 3T3 cells (Table 1). However, by using a targeted MS approach using a list of precursors that were generated on the basis of the unmodified and modified peptides of interest, we were able to detect Tyr^{307}-phosphorylated peptides in two of two repeats of the HA-PP2A$_C$ immunoprecipitates from EGF/PV-treated NIH 3T3 cells (Table1; Table S1), indicating that pTyr307 exists but likely at very low abundance, as suggested by the low peptide intensities compared with the unmodified counterpart (Table S2).

Commercial "PP2A$_C$ pTyr^{307}" Antibodies Are Not Specific for pTyr^{307} and Display Cross-Reactivity with the Tyr Phosphorylated Hemagglutinin Tag

To further investigate the specificity of the commercial "PP2A$_C$ pTyr^{307}" antibodies, we performed an ELISA using synthetic C-terminal PP2A$_C$ undecapeptides that were either unphosphorylated or phosphorylated on Tyr^{307}. We also checked for potential cross-reactivity with the Tyr-phosphorylated HA-epitope tag (phosphorylated on tyrosine 2, 4, or 9), which shows some sequence similarity to the PP2A$_C$ C terminus (Figure 1C). The general pTyr antibody 4G10 specifically detected Tyr-phosphorylated PP2A$_C$ and HA peptides. Detection of the HA tag by antibody 12CA5, which we used in the immunoprecipitation experiments, was hampered by phosphorylation on Tyr^9 but not on Tyr^2 and Tyr^4. Detection by the HA antibody 16B12, which was

deviation of at least three independent experiments. The signals were normalized to pTyr^{307} peptide, which was arbitrarily set to 1. Data are represented as mean ± SD. Statistical significance was assessed using ANOVA followed by Tukey's honestly significant difference (HSD) test as a post hoc test: *$p < 0.05$, **$p < 0.01$, and ***$p < 0.001$. NS, not significant.
See also Figure S1 and Tables S1 and S2.

Table 1. C-Terminal PP2A$_C$ Peptides Covering the Sites of Interest that Were Identified Using LC-MS in the Described Experimental Setups

Phosphorylation Site	Peptide	NIH 3T3 HA-C vSrc + PV	NIH 3T3 HA-C + PV/EGF	HEK293T Myc C, + Src^{CA}	Site Probability	Best Score	Mass Accuracy (ppm)
PPP2ca							
T304	_RT(ph)PDYFL_	+	+	+	0.999	118.33	0.91
T304	_RT(ph)PDYFL_(me)	+	+	+	1	100.98	−0.18
Y307	_RTPDY(ph)FL_	–	+	+	1	110.3	−0.05
Y307	_RTPDY(ph)FL_(me)	–	+	+	0.999	89.7	0.27
HA-Tag							
Y4	_M(ox)YPY(ph)DVPDYALVPR_	+	+	N/A	1	149.96	0.09
Y9	_M(ox)YPYDVPDY(ph)ALVPR_	+	–	N/A	1	229.53	−0.32

Peptides covering the sites of interest that were identified using LC-MS in the described experimental setups (+). Peptides covering the HA-tag are not applicable (N/A) to the Myc C experiment. Best score is the Andromeda score for the best identified MS/MS spectrum of the corresponding peptide. (ph) and (me) stand for phosphorylation and methylation, respectively. See also Figure S2 and Tables S1 and S2.

used in all western experiments, was decreased by Tyr^2 phosphorylation and increased by Tyr^9 phosphorylation compared with the unphosphorylated tag sequence (Figure 1D). The rabbit monoclonal E155 detected the unphosphorylated and Tyr^{307}-phosphorylated PP2A$_C$ C terminus equally well and did not cross-react with the tyrosine-phosphorylated HA peptides. The mouse monoclonal F-8 antibody (from SCBT) showed almost identical detection properties to clone E155 (Figures 1D and S1C). The rabbit polyclonal antibodies (from SCBT and R&D Systems) gave substantial signals on the unmodified PP2A$_C$ C-terminal peptide and 5.9- and 1.9-fold increased signal, respectively, on the pTyr^{307} peptide compared with the unphosphorylated peptide. However, both antibodies cross-reacted with the phosphorylated HA tag peptides, particularly those with pTyr^9, whose surrounding sequence is similar to PP2A$_C$ pTyr^{307} (Figures 1D and S1B) and which we identified in an MS phosphopeptide analysis of EGF/PV-treated v-src transformed NIH 3T3 cells (Table 1). The monoclonal 4B10 antibody and the SCBT goat polyclonal antibody recognized phosphorylated Tyr^{307} but also cross-reacted with the HA-tag phosphorylated at Tyr^9 (Figure S1B). A recently marketed rabbit polyclonal pTyr^{307} antibody (from Sigma-Aldrich) was the only antibody that recognized the pTyr^{307} peptide but not the phosphorylated HA peptides (Figure 1D).

Phosphorylation of PP2A$_C$ on Tyr^{307} Can Be Detected Using MS after Transient Overexpression of PP2A$_C$ and Constitutively Active Src

Besides stimulation with EGF, Src has been reported to phosphorylate PP2A$_C$ on Tyr^{307} *in vitro* (Chen et al., 1994) and in cells using "PP2A$_C$ pTyr^{307}" antibodies (Hu et al., 2009). However, it is important to point out that thus far, the existence of this site has never been validated using MS (PhosphoSitePlus, https://www.phosphosite.org/homeAction.action), and we were only able to detect pTyr^{307} at very low abundance in EGF/PV-stimulated cells (Tables 1, S1, and S2). To test for the existence of Src-dependent PP2A phosphorylation at Tyr^{307}, we transiently overexpressed the constitutively active Src mutant, Y529F (Src^{CA}) (Luo et al., 2008) together with Myc-tagged PP2A$_C$ in HEK293T cells and then performed MS analyses of the Myc immune complexes. Under these specific experimental conditions, we were able to detect reliably the pTyr^{307} site; however, phosphorylation of this site was not observed in HEK293T cells that did not overexpress Src^{CA} or PP2A$_C$ (Figures S2A and S2B; Tables 1, S1, and S2).

The Putative Src^{CA}-Dependent Phosphorylation of PP2A$_C$ on Tyr^{307} Is Not Reliably Detected by Most "PP2A$_C$ pTyr^{307}" Antibodies

On the basis of the MS identification of the pTyr^{307} site in cells transiently co-expressing PP2A$_C$ and Src^{CA}, we next evaluated the specificity of "PP2A$_C$ pTyr^{307}" antibodies in this model. We overexpressed either HA- or myc-tagged wild-type PP2A$_C$ subunits or myc-PP2A$_C$ Y307F mutant as a negative control. If the "PP2A$_C$ pTyr^{307}" antibodies were indeed specific, we would have expected an increased signal of wild-type PP2A$_C$ following transient Src^{CA} expression. However, despite increased global tyrosine phosphorylation, we did not detect increased signals using either E155 or F-8 "PP2A$_C$ pTyr^{307}" antibodies; rather, Src overexpression caused a 30% decrease in the myc-PP2A$_C$ signal (Figure 2A). The R&D Systems and Thermo Fisher Scientific pTyr^{307} rabbit polyclonal antibodies showed increased signals upon Src^{CA} expression, but substantial signals were also observed using the Y307F mutant and after CIP treatment (Figure 2B; Figures S3A and S3B), indicating a lack of specificity of these antibodies.

At first glance, the Sigma-Aldrich and SCBT polyclonal rabbit pTyr^{307} antibodies appeared to be more specific for pTyr^{307}, as neither of these antibodies detected the PP2A$_C$ Y307F mutant or the wild-type PP2A$_C$ subunit without concomitant Src^{CA} expression, and moreover, the phospho-specific signal was almost completely abolished after dephosphorylation by CIP (Figures 2A and 2B; Figures S3A and S3B). However, many cross-reactive bands were recognized by these antibodies in Src^{CA} overexpressing cells, suggesting general pTyr cross-reactivity. In the case of the SCBT rabbit polyclonal, this cross-reactivity probably also extended to the Tyr-phosphorylated HA epitope tag (Figure S1B). With the 4B10 monoclonal and also with the SCBT goat polyclonal antibody (lot A2413), we observed a Src^{CA}-dependent increase in the immunoreactivity of HA-PP2A$_C$

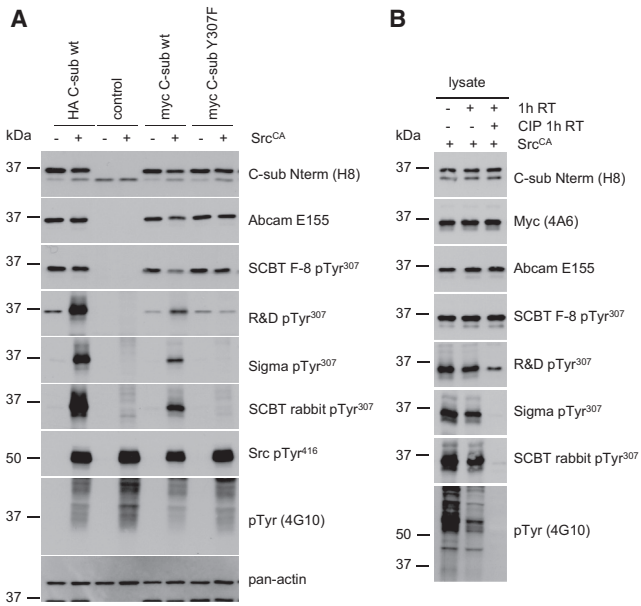

Figure 2. "PP2A$_C$ pTyr^{307}" Antibodies Display Different Immunoreactivity toward PP2A$_C$ in Cells Co-expressing Src^{CA} and Tagged PP2A$_C$ Subunit

(A) Immunoblotting of lysates of HEK293T cells transiently transfected with pcDNA3 puro HA C-sub wild-type (WT), pcDNA3 puro, pcDNA3 puro myc C-sub WT, or pcDNA3 puro myc C-sub Y307F, co-transfected with (+) or without (–) pRC/CMV Src^{Y529F} using the indicated antibodies. The panels originate from eight different blotting membranes; the H8 blot was reincubated with pan-actin antibody. The blots are representative of three independent experiments.

(B) Immunoblotting of lysates of HEK293T cells transiently co-transfected with pcDNA3 puro myc C-sub WT and pRC/CMV Src^{Y529F} using the indicated antibodies. Lysates were either directly boiled or treated with CIP or vehicle before boiling. The panels originate from eight different blotting membranes. The blots are representative of three independent experiments.

See also Figure S3.

and to a much lesser extent of Myc-PP2A$_C$; however, the increased signals were only detectable at extended exposure times (Figure S3A). Surprisingly, western analyses revealed that a previous lot (lot L0413) of the SCBT goat antibody recognized PP2A$_C$ strongly and equally well in total lysates from control as well as Src^{CA}-expressing and/or PV-treated COS-7 cells, but this signal was also insensitive to alkaline phosphatase treatment (Figure S1D). These findings indicated a dramatic lot-to-lot variation of antibody properties. The goat polyclonal antibody was discontinued by SCBT at the end of 2017 and thus cannot be further investigated. Nonetheless, our results should be kept in mind when researchers revisit findings generated with the different lots of this antibody.

All "PP2A$_C$ pTyr^{307}" Antibodies Are Affected by PP2A$_C$ Methylation on Leu^{309}

Commercial "PP2A$_C$ pTyr^{307}" antibodies have been used in >180 publications for the detection of Tyr^{307} phosphorylation levels because pTyr^{307} levels are thought to be a direct readout for the amount of inhibited PP2A in cells and tissues. In particular, the high levels of pTyr^{307} detected in some cancer cells were interpreted as inactivation of PP2A's tumor suppressor function following hyperactivation of tyrosine kinase pathways (Chen et al., 2017; Cristóbal et al., 2014a, 2014c; Rincón et al., 2015; Roberts et al., 2010; Velmurugan et al., 2018). Because our data indicated that most commercial "pTyr^{307}" antibodies were not specific for pTyr^{307}, the question arose as to what changes these antibodies were detecting in the targeted C-terminal epitope.

In mammalian cells, up to 90% of PP2A$_C$ is carboxymethylated on Leu^{309} at the C-terminal tail (Yu et al., 2001). We also observed that PP2A$_C$ can be phosphorylated on Thr^{304} (Figures S2C and S2D; Schmitz et al., 2010). Significantly, both modifications can influence the binding of antibodies directed toward the PP2A$_C$ C terminus (Frohner et al., 2020). To check whether these modifications influence the binding of the "PP2A$_C$ pTyr^{307}" antibodies, we performed ELISAs using C-terminal undecapeptides that were either nonmethylated or Leu^{309} methylated and, in addition, either phosphorylated or non-phosphorylated at Tyr^{307} or Thr^{304} sites. Leu^{309} carboxymethylation markedly impaired recognition of the unphosphorylated C-terminal peptide by the E155 and F-8 monoclonal antibodies. Although F-8 was also impaired on the double-modified peptide, E155 showed only a 60% signal reduction compared with the unmodified peptide (Figure 3A). The R&D Systems polyclonal antibody showed detection properties similar to E155, but its methylation sensitivity was almost completely nullified by Tyr^{307} phosphorylation. This binding behavior can probably be explained by the polyclonal nature of antiserum, which likely contains methylation-sensitive, non-pTyr^{307}-specific antibodies as well as pTyr^{307}-specific, methylation-insensitive antibodies. The Sigma-Aldrich polyclonal antibody again showed the highest specificity for pTyr^{307} and exhibited only a slight methylation sensitivity, indicated by a 26% signal reduction on the methylated pTyr^{307} peptide (Figure 3A). The recognition of pTyr^{307} by monoclonal antibody 4B10 was completely hampered by concomitant methylation. Conversely, recognition of pTyr^{307} by the SCBT rabbit and goat polyclonal antibodies was minimally altered by Leu^{309} methylation. The cross-reactivity of the SCBT rabbit antibody with the unphosphorylated PP2A$_C$ C terminus, however, was also substantially reduced by Leu^{309} carboxymethylation (Figure S4A). Furthermore, we tested whether phosphorylation of Thr^{304} had any influence on PP2A$_C$ recognition by the E155, F-8, or R&D Systems antibodies (Figure S4B). The E155 signal decreased by 30% when Thr^{304} was phosphorylated and was completely abolished when the peptide was additionally methylated. The F-8 antibody only recognized the nonmethylated peptide, and phosphorylation of Thr^{304} abolished binding. Likewise, the R&D Systems antibody did not recognize the methylated peptides; however, the signal was not influenced by Thr^{304} phosphorylation (Figure S4B). These data indicated that PP2A$_C$ signal changes reported in the literature with the E155 and F-8 monoclonal antibodies are due to changes in the methylation and/or Thr^{304} phosphorylation levels rather than changes in the phosphorylation state of the claimed target, Tyr^{307}.

To further explore the role of PP2A$_C$ carboxymethylation on antibody specificity, we first performed a western blot analysis

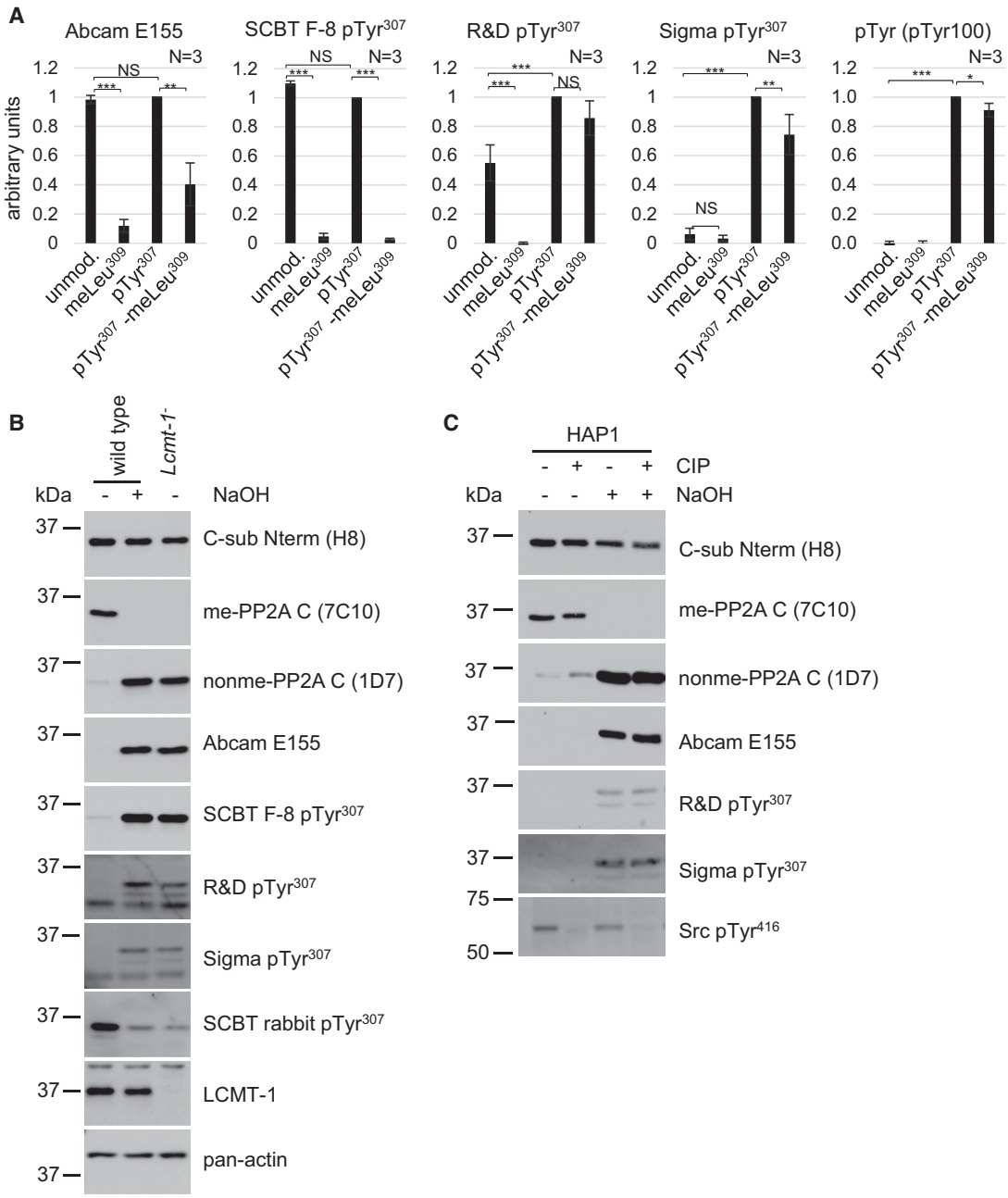

Figure 3. Cross-Reactivity and Non-specificity of Commercial "PP2A$_C$ pTyr^{307}" Antibodies

(A) Quantification of binding of the indicated antibodies to peptides unmod (HVTRRTPDYFL), meLeu^{309} (HVTRRTPDYFL-me), pTyr^{307} (HVTRRTPDpYFL), and pTyr^{307}-meLeu^{309} (HVTRRTPDpYFL-me). Antibody binding data are shown as the average and standard deviation of three independent experiments. The signals were normalized to the pTyr^{307} peptide for Tyr antibodies, which were arbitrarily set to 1. Data are represented as mean ± SD. Statistical significance was assessed using ANOVA (followed by Tukey's HSD test as a post hoc test): *$p < 0.05$, **$p < 0.01$, and ***$p < 0.001$. NS, not significant.

(B) Immunoblotting of lysates of HAP1 wild-type cells that were either directly boiled or treated with NaOH before boiling, and of HAP1 *Lcmt-1*$^{-}$ cells directly boiled with the indicated antibodies. Panels originate from eight different blotting membranes. The blots are representative of three independent experiments.

(C) Immunoblotting of lysates of HAP1 wild-type cells either directly boiled or treated CIP or NaOH or NaOH and CIP using the indicated antibodies. Panels originate from six different blotting membranes. The 7C10 blot was reincubated with Src pTyr^{416}. The blots are representative of three independent experiments. See also Figure S4.

of HAP1 wild-type cells that are near-haploid derivates of the chronic myelogenous leukemia cell line KBM-7 (Kotecki et al., 1999). The cell lysates were either untreated or treated with NaOH to chemically remove the methyl group from the cellular pool of methylated PP2A$_C$ (Favre et al., 1994). In parallel, we analyzed lysates of HAP1 cells lacking the PP2A$_C$

methyltransferase *Lcmt-1*, which results in accumulation of non-methylated $PP2A_C$ (Hwang et al., 2016). The E155, F-8, and R&D Systems signals increased in lysates from NaOH-treated and *Lcmt-1*$^{-}$ cells compared with untreated HAP1 wild-type cells, thereby confirming the methylation sensitivity of these antibodies (Figure 3B). Likewise, the methylation sensitivity of the most widely used E155 antibody was also confirmed in N2a cells (Figure S1E). In contrast to what was observed with the E155, F-8, and R&D Systems antibodies, the SCBT rabbit signal decreased upon demethylation with NaOH and in *Lcmt-1*$^{-}$ HAP1 cell lysates (Figure 3B); this observation contrasts with the ELISA data showing that the SCBT rabbit antibody was slightly hampered by meLeu^{309} (Figure S4A). Unexpectedly, the Sigma-Aldrich pTyr^{307} antibody detected nonmethylated $PP2A_C$ upon NaOH treatment of HAP1 cells or in *Lcmt-1*$^{-}$ cells, but it failed to detect $PP2A_C$ in untreated HAP1 wild-type cells wherein >90% of endogenous $PP2A_C$ was methylated (Figure 3B). The absence of a signal in the untreated HAP1 wild-type cells also suggested that Tyr^{307} is probably not phosphorylated in these cells. Furthermore, parallel incubation of NaOH-treated and untreated HAP1 lysates with CIP to remove phosphate groups did not decrease the signal generated by the Sigma-Aldrich, R&D Systems, or E155 antibodies, confirming the cross-reactivity with the unmodified $PP2A_C$ C terminus (Figure 3C).

Monoclonal E155 Does Not Detect SET-Mediated Phosphorylation of PP2Ac at Tyr^{307} upon Activation of Conventional T Cells

SET (inhibitor 2 of PP2A/I2PP2A) is a potent inhibitor of PP2A, and its overexpression contributes to the pathogenesis of hematological malignancies (Arriazu et al., 2016). The predominant model of how SET inactivates PP2A *in vivo* is based almost exclusively on the use of E155 and claims that SET inhibits PP2Ac by increasing the phosphorylation of Tyr^{307}(Cristóbal et al., 2010, 2011; Inoue et al., 2015; Kake et al., 2017; Kawashima and Kirito, 2016; Lucas et al., 2011, 2018; Neviani et al., 2005; Oaks et al., 2013; Piazza et al., 2013; Richard et al., 2016). Representative for this model, we re-evaluated data from a recent study in which E155 was used to show that activation of conventional T cells leads to SET-mediated phosphorylation and inhibition of PP2A (Apostolidis et al., 2016). In agreement with that study, we found a 2-fold induction of SET after 24 h of T cell activation with CD3 and CD28 antibodies and no changes in the abundance of the total $PP2A_C$ levels (Figures 4A and 4B). Under experimental conditions that conserve the $PP2A_C$ methylation level (Yabe et al., 2018) we observed, in contrast to the published data, a 2.3-fold decrease of the signal with E155 in the activated T cells, a decrease with a methyl-sensitive antibody, clone 1D7, and a reciprocal increase with the methyl-specific antibody clone 7C10 (Figures 4B and 4C). NaOH treatment of the lysates led to equal E155 and 1D7 signals in the unstimulated and stimulated T cells and confirmed the methylation sensitivity of these antibodies (Figure 4B). Phosphatase treatment of the lysates led to substantial dephosphorylation of SET but did not change the E155 signal intensities, as expected from an antibody that has no specificity for pTyr^{307} (Figure 4B). Furthermore, we did not observe a signal, in neither the unstimulated nor the stimulated T cells, with the polyclonal pTyr^{307} antibody from Sigma-Aldrich (Figure 4B), which possessed the highest pTyr307 specificity. Thus, the observed changes in E155 signals upon T cell activation correspond to changes in PP2Ac methylation but not pTyr^{307} phosphorylation.

DISCUSSION

The excellent intrinsic properties and versatile use in many research applications make antibodies the most often used tools in the life sciences. Antibodies are easy to generate, and >2 million antibodies are available from >300 commercial sources, generating sales of $2.7 billion in 2016, according to a 2017 report published by the digital marketplace Biocompare (https://www.biocompare.com/). At the same time, antibodies have been identified as a prime cause for what is called the reproducibility crisis (Baker, 2015). In our study, we identified $PP2A_C$ pTyr^{307} antibodies as yet another example of this crisis. Our thorough analyses of eight commercial $PP2A_C$ pTyr^{307} antibodies revealed that the most frequently used antibodies, E155 and F-8, were not specific at all for the pTyr^{307} site, and all tested antibodies showed various degrees of cross-reactivity or sensitivities to other post-translational modifications at nearby sites.

What are the reasons that these problems with pTyr^{307} antibodies went unnoticed for such a long time? A major reason was, and still is, the lack of proper validation of pTyr^{307} antibodies. Simple and absolutely necessary controls such as ablating the signal with phosphatase treatment of lysates or determining the general protein and $PP2A_C$ levels with suitable control antibodies were not carried out. Phosphatase treatment would have at least revealed a general phospho-specificity of the antibody, but not necessarily its $PP2A_C$ pTyr^{307} site specificity. This would have required an ELISA or dot-blot assay with the phosphorylated/unphosphorylated immunogen peptide compared with other phosphorylated/unphosphorylated control peptides. Unfortunately, these controls were not included in the E155 data specifications from Epitomics. Likewise, the R&D Systems polyclonal pTyr^{307} antibody was validated only using western blot analysis, again without any phosphatase-treated control. The quality control (QC) of other antibodies, including the SCBT poly- and monoclonal antibodies included such a control, but phosphatase treatment only reduced and did not completely abolish the signal as it should for a truly phospho-specific antibody (i.e., under the assumption that the phosphatase treatment had worked efficiently). However, the seemingly reduced phospho-specific signal in the phosphatase control was most likely due to unequal loading of lysates (https://www.scbt.com/scbt/p/p-pp2a-calpha-beta-antibody-f-8), because the signals generated by the $PP2A_C$ loading control antibody 1D6 seem to fluctuate in a similar manner (although overexposed signals hardly allow proper quantification). The interpretation of the data is further complicated by the fact that the loading control antibody 1D6 is also directed against the $PP2A_C$ C terminus, and our recent work revealed that recognition of PP2A by 1D6 is hampered by methylation and, even more important, by Tyr^{307} phosphorylation (Frohner et al., 2020). Only the recently marketed polyclonal pTyr^{307} antibody from Sigma-Aldrich and the mouse monoclonal antibody 4B10 that was generated and

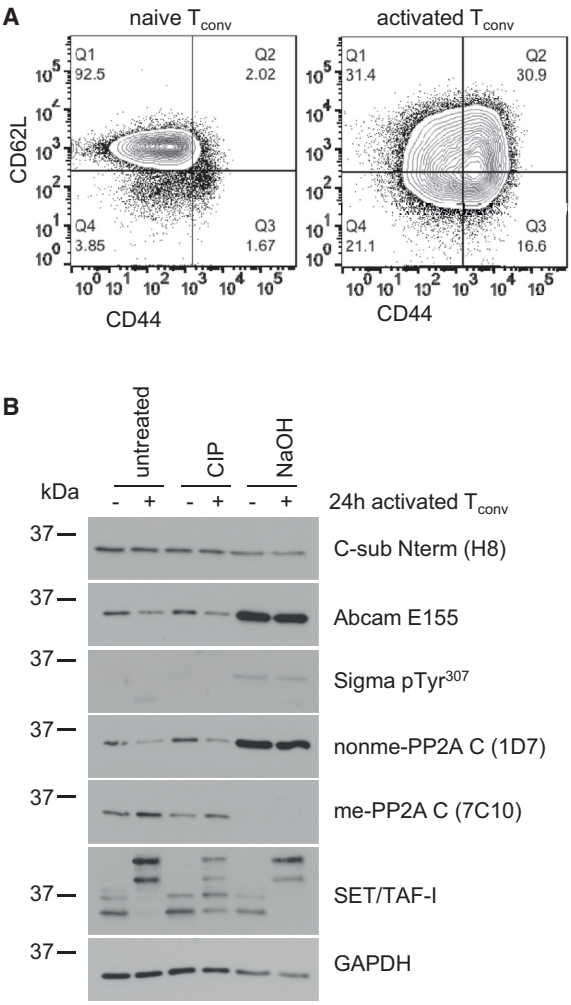

Figure 4. Monoclonal E155 Does Not Detect SET-Mediated Phosphorylation of PP2Ac at Tyr^{307} upon Activation of Conventional T Cells

(A) Naive and activated CD4+ T cells were stained for CD62L and CD44 followed by flow cytometry analysis.

(B) Immunoblotting of lysates of CD4$^+$ T cells, naive (–) and activated for 24 h (+) normalized to total protein amount, either left untreated or treated with CIP or NaOH before boiling. Panels originate from five different blotting membranes. The 7C10 blot was reincubated with SET/TAF-I and the Sigma-Aldrich blot with GAPDH. The blots are representative of N = 3 independent T cell isolation and immunoblotting experiments.

(C) The SET, E155, 1D7, and 7C10 signals were quantified from three independent experiments relative to H8 (PP2A$_C$) or GAPDH signals. Data are represented as mean ± SD. Statistical significance was assessed using ANOVA (followed by Tukey's HSD as a post hoc test: *p < 0.05, **p < 0.01, and ***p < 0.001. NS, not significant.

characterized by our lab were properly validated by peptide ELISAs for their pTyr^{307} specificity.

Lot-to-lot variability of commercial antibodies, in particular polyclonal antibodies, has been identified as one of the causes for their unreliability and has led to the claim that only recombinant binding reagents with defined sequence should be used for the detection of proteins (Baker, 2015). Because of the intrinsic nature of the immune response, a polyclonal antiserum is an undefined mixture of antibodies, whose composition and affinities change during the course of immunization, and the difference in the immune response between different laboratory animals is even larger. These issues raise significant concerns about the use of polyclonal antisera as reliable tools for the specific detection of post-translationally modified amino acids such as the pTyr^{307}. Not surprisingly, all tested polyclonal pTyr^{307} antibodies showed various degrees of cross- and off-target site reactivities. What makes the problem even worse is the lack of lot-to-lot QC and validation. This practice of not validating antibody batches goes so far that the exact same figure that was shown on the datasheet of previous lots is presented as the validation figure for new lots.

How can the validation practice be changed? First and foremost, scientists, grant organizations, and publishers must demand that commercial antibodies be validated with the highest possible, financially feasible standards, a demand already put forward in 2015 (Bradbury and Plückthun, 2015). Clearly, research antibodies with yearly sales of a few thousand dollars cannot be characterized and optimized in the same manner and depth as therapeutic antibodies with yearly revenues of several billion dollars. However, a catalog of guidelines that must be fulfilled by companies to help buyers assess the validation level of an immunochemical reagent has been suggested (Roncador et al., 2016; Taussig et al., 2018; Weller, 2018). The more we know about the antibody properties the better. However, even if all these criteria are met, we could still encounter some unforeseen issues. For example, in case of the PP2A$_C$ C terminus with three modified amino acids within a range of six amino acids, it might be difficult, if not impossible, to generate an antibody that is specific for only one modified site and is not influenced at all by the modification of the neighboring residues. What we can do, however, is determine the impact of these modifications on the recognition of the targeted site and with this knowledge use the antibody with the necessary control experiments. For example, phosphatase treatment, alone or in combination with the chemical removal of the PP2A$_C$ carboxymethylation, should reveal the amount of background signal that can be expected when using the polyclonal pTyr^{307} antibody from Sigma-Aldrich.

The consequences of using badly validated antibodies are far reaching (Begley and Ellis, 2012), and the losses in terms of time and resources are dramatic. Two decades of PP2A research, in particular on its role as a tumor suppressor, followed a model in which the tumor suppressor function of PP2A was thought to become inhibited by the phosphorylation of Tyr^{307}. However, on the basis of our and the accompanying paper's results (Mazhar et al., 2020 [this issue of *Cell Reports*]), this hypothesis should be doubted if monoclonal antibodies E155 and F-8 were used, because any signal increase detected with these two antibodies was due to an increase in the fraction of demethylated $PP2A_C$ but not Tyr^{307}-phosphorylated $PP2A_C$. Interestingly, increased demethylation has been found in endometrial cancer and glioma cells (Kaur et al., 2016; Wandzioch et al., 2014), and the reduction of $PP2A_C$ methylation in human cells has been shown to enhance their transformation in an Akt-dependent manner (Jackson and Pallas, 2012), suggesting a tumor-suppressive function of methylation-dependent PP2A holoenzymes. All studies published with the methyl-sensitive antibodies E155 and F-8 (see "Mendeley: list of publications using commercial $PP2A_C$ $pTyr^{307}$ antibodies") had therefore identified the dysregulation of $PP2A_C$ methylation and not, as was believed, the hyperphosphorylation of $PP2A_C$. In particular, those studies that suggest using $pTyr^{307}$ levels as a prognostic or predictive biomarker must be reinterpreted by readers in light of the findings from our and Narla's groups (Chen et al., 2017; Cristóbal et al., 2011. 2014b, 2019; Lucas et al., 2018; Rincón et al., 2015). The interpretation of results obtained with the polyclonal $pTyr^{307}$ antibodies is even more complex and almost impossible given the antibodies' multiple cross-reactivities and unclear lot-to-lot variabilities.

Is $PP2A_C$ Tyr^{307} a bona fide phospho-acceptor site, and if so, what are the functional consequences of this modification? Almost all studies conducted since the initial reports used faulty antibodies for $pTyr^{307}$ detection. Therefore, the PP2A field must go back and revisit the original findings. Mutational analysis of this site indicated a role in holoenzyme assembly (Longin et al., 2007; Nunbhakdi-Craig et al., 2007; Ogris et al., 1997). Here, we could reliably detect Tyr^{307} phosphorylation only under supra-physiological conditions, with transient overexpression of active Src and $PP2A_C$ subunit. The physiological conditions under which phosphorylation of $pTyr^{307}$ occurs are unknown, and the biological relevance and function of this post-translational modification are still unclear. New and better detection tools for PP2A $pTyr^{307}$ are critically needed to shed light on the stoichiometry and significance of this mystery site.

STAR★METHODS

Detailed methods are provided in the online version of this paper and include the following:

SUPPLEMENTAL INFORMATION

Supplemental Information can be found online at https://doi.org/10.1016/j.celrep.2020.02.035.

ACKNOWLEDGMENTS

We thank Dr. David Virshup, Duke-NUS Medical School (Singapore), for critically reading the manuscript and Dr. John Alberta and Dr. Thomas Roberts, Dana-Farber Cancer Institute (DFCI), Harvard Medical School (Boston), for materials. MS analyses were performed at the Mass Spectrometry Facility of Max Perutz Labs Vienna using the Vienna BioCenter Core Facilities (VBCF) instrument pool. This work was funded by service and royalty fees from antibody licensing agreements and the monoclonal antibody service facility (E.O. lab), and was partially supported by grant G1700055 from the Hunter Medical Research Institute (New South Wales, Australia) (E.S. and J.-M.S.).

AUTHOR CONTRIBUTIONS

I.E.F conceived, performed, and analyzed experiments, prepared figures, and wrote the manuscript. S.S., I.M., T.P., and J.-M.S. performed and analyzed experiments. E.S. conceived and analyzed experiments and prepared figures. D.A. and M.H. performed liquid chromatography (LC)-MS experiments and data analysis and revised the manuscript. B.E.W., E.S., and W.E. revised the manuscript. E.O. conceived and analyzed experiments and wrote the manuscript.

DECLARATION OF INTERESTS

E.O. serves as a consultant to Millipore Corporation. Monoclonal antibody 4B10 against Tyr^{307}-phosphorylated $PP2A_C$ subunit is licensed to the biotech companies BioLegend/Covance, BioTechne/Novus, EMD Millipore (discontinued), and SCBT. Monoclonal antibody 1D7 against nonmethylated $PP2A_C$ subunit is licensed to BioLegend/Covance. Monoclonal antibody 4A6 against the myc epitope tag is licensed to EMD Millipore. Monoclonal antibody 2A3 against pan-actin is licensed to the biotech companies EMD Millipore and SCBT. The authors confirm that they will adhere to all the policies of *Cell Reports* on sharing data and materials. The Medical University of Vienna on behalf of E.O. is filing a patent on the PP2A methyl-C subunit-specific monoclonal antibody 7C10.

Received: October 29, 2019
Revised: December 3, 2019
Accepted: February 7, 2020
Published: March 3, 2020

REFERENCES

Apostolidis, S.A., Rodríguez-Rodríguez, N., Suárez-Fueyo, A., Dioufa, N., Ozcan, E., Crispín, J.C., Tsokos, M.G., and Tsokos, G.C. (2016). Phosphatase PP2A is requisite for the function of regulatory T cells. Nat. Immunol. *17*, 556–564.

Arriazu, E., Pippa, R., and Odero, M.D. (2016). Protein phosphatase 2A as a therapeutic target in acute myeloid leukemia. Front. Oncol. *6*, 78.

Baker, M. (2015). Reproducibility crisis: blame it on the antibodies. Nature *521*, 274–276.

Begley, C.G., and Ellis, L.M. (2012). Drug development: raise standards for preclinical cancer research. Nature *483*, 531–533.

Bradbury, A.M., and Plückthun, A. (2015). Antibodies: validate recombinants once. Nature *520*, 295.

Brautigan, D.L. (2013). Protein Ser/Thr phosphatases—the ugly ducklings of cell signalling. FEBS J. *280*, 324–345.

Chen, J., Martin, B.L., and Brautigan, D.L. (1992). Regulation of protein serine-threonine phosphatase type-2A by tyrosine phosphorylation. Science *257*, 1261–1264.

Chen, J., Parsons, S., and Brautigan, D.L. (1994). Tyrosine phosphorylation of protein phosphatase 2A in response to growth stimulation and v-src transformation of fibroblasts. J. Biol. Chem. *269*, 7957–7962.

Chen, P.M., Chu, P.Y., Tung, S.L., Liu, C.Y., Tsai, Y.F., Lin, Y.S., Wang, W.L., Wang, Y.L., Lien, P.J., Chao, T.C., and Tseng, L.M. (2017). Overexpression of phosphoprotein phosphatase 2A predicts worse prognosis in patients with breast cancer: a 15-year follow-up. Hum. Pathol. *66*, 93–100.

Cox, J., and Mann, M. (2008). MaxQuant enables high peptide identification rates, individualized p.p.b.-range mass accuracies and proteome-wide protein quantification. Nat. Biotechnol. *26*, 1367–1372.

Cristóbal, I., Blanco, F.J., Garcia-Orti, L., Marcotegui, N., Vicente, C., Rifon, J., Novo, F.J., Bandres, E., Calasanz, M.J., Bernabeu, C., and Odero, M.D. (2010). SETBP1 overexpression is a novel leukemogenic mechanism that predicts adverse outcome in elderly patients with acute myeloid leukemia. Blood *115*, 615–625.

Cristóbal, I., Garcia-Orti, L., Cirauqui, C., Alonso, M.M., Calasanz, M.J., and Odero, M.D. (2011). PP2A impaired activity is a common event in acute myeloid leukemia and its activation by forskolin has a potent anti-leukemic effect. Leukemia *25*, 606–614.

Cristóbal, I., Manso, R., Rincón, R., Caramés, C., Senin, C., Borrero, A., Martínez-Useros, J., Rodriguez, M., Zazo, S., Aguilera, O., et al. (2014a). PP2A inhibition is a common event in colorectal cancer and its restoration using FTY720 shows promising therapeutic potential. Mol. Cancer Ther. *13*, 938–947.

Cristóbal, I., Manso, R., Rincón, R., Caramés, C., Zazo, S., Del Pulgar, T.G., Cebrián, A., Madoz-Gúrpide, J., Rojo, F., and García-Foncillas, J. (2014b). Phosphorylated protein phosphatase 2A determines poor outcome in patients with metastatic colorectal cancer. Br. J. Cancer *111*, 756–762.

Cristóbal, I., Rincón, R., Manso, R., Madoz-Gúrpide, J., Caramés, C., del Puerto-Nevado, L., Rojo, F., and García-Foncillas, J. (2014c). Hyperphosphorylation of PP2A in colorectal cancer and the potential therapeutic value showed by its forskolin-induced dephosphorylation and activation. Biochim. Biophys. Acta *1842*, 1823–1829.

Cristóbal, I., Torrejón, B., Rubio, J., Santos, A., Pedregal, M., Caramés, C., Zazo, S., Luque, M., Sanz-Alvarez, M., Madoz-Gúrpide, J., et al. (2019). Deregulation of SET is associated with tumor progression and predicts adverse outcome in patients with early-stage colorectal cancer. J. Clin. Med. *8*, 346.

Damuni, Z., Xiong, H., and Li, M. (1994). Autophosphorylation-activated protein kinase inactivates the protein tyrosine phosphatase activity of protein phosphatase 2A. FEBS Lett. *352*, 311–314.

Du, T.T., Wang, L., Duan, C.L., Lu, L.L., Zhang, J.L., Gao, G., Qiu, X.B., Wang, X.M., and Yang, H. (2015). GBA deficiency promotes SNCA/α-synuclein accumulation through autophagic inhibition by inactivated PPP2A. Autophagy *11*, 1803–1820.

Du, T.T., Chen, Y.C., Lu, Y.Q., Meng, F.G., Yang, H., and Zhang, J.G. (2018). Subthalamic nucleus deep brain stimulation protects neurons by activating autophagy via PP2A inactivation in a rat model of Parkinson's disease. Exp. Neurol. *306*, 232–242.

Dudiki, T., Kadunganattil, S., Ferrara, J.K., Kline, D.W., and Vijayaraghavan, S. (2015). Changes in carboxy methylation and tyrosine phosphorylation of protein phosphatase PP2A are associated with epididymal sperm maturation and motility. PLoS ONE *10*, e0141961.

Favre, B., Zolnierowicz, S., Turowski, P., and Hemmings, B.A. (1994). The catalytic subunit of protein phosphatase 2A is carboxyl-methylated in vivo. J. Biol. Chem. *269*, 16311–16317.

Fellner, T., Lackner, D.H., Hombauer, H., Piribauer, P., Mudrak, I., Zaragoza, K., Juno, C., and Ogris, E. (2003). A novel and essential mechanism determining specificity and activity of protein phosphatase 2A (PP2A) in vivo. Genes Dev. *17*, 2138–2150.

Frohner, I.E., Mudrak, I., Kronlachner, S., Schüchner, S., and Ogris, E. (2020). Antibodies recognizing the C terminus of PP2A catalytic subunit are unsuitable for evaluating PP2A activity and holoenzyme composition. Sci. Signal. *13*, eaax6490.

Green, N., Alexander, H., Olson, A., Alexander, S., Shinnick, T.M., Sutcliffe, J.G., and Lerner, R.A. (1982). Immunogenic structure of the influenza virus hemagglutinin. Cell *28*, 477–487.

Gu, T.L., Deng, X., Huang, F., Tucker, M., Crosby, K., Rimkunas, V., Wang, Y., Deng, G., Zhu, L., Tan, Z., et al. (2011). Survey of tyrosine kinase signaling reveals ROS kinase fusions in human cholangiocarcinoma. PLoS ONE *6*, e15640.

Gu, Y., Barzegar, M., Chen, X., Wu, Y., Shang, C., Mahdavian, E., Salvatore, B.A., Jiang, S., and Huang, S. (2015). Fusarochromanone-induced reactive oxygen species results in activation of JNK cascade and cell death by inhibiting protein phosphatases 2A and 5. Oncotarget *6*, 42322–42333.

Guo, H., and Damuni, Z. (1993). Autophosphorylation-activated protein kinase phosphorylates and inactivates protein phosphatase 2A. Proc. Natl. Acad. Sci. U S A *90*, 2500–2504.

Hombauer, H., Weismann, D., Mudrak, I., Stanzel, C., Fellner, T., Lackner, D.H., and Ogris, E. (2007). Generation of active protein phosphatase 2A is coupled to holoenzyme assembly. PLoS Biol. *5*, e155.

Hu, X., Wu, X., Xu, J., Zhou, J., Han, X., and Guo, J. (2009). Src kinase up-regulates the ERK cascade through inactivation of protein phosphatase 2A following cerebral ischemia. BMC Neurosci. *10*, 74.

Huang, P., Wang, B., Wang, X., Xing, M., Guo, Z., and Xu, L. (2017). HEK293 cells exposed to microcystin-LR show reduced protein phosphatase 2A activity and more stable cytoskeletal structure when overexpressing α4 protein. Environ. Toxicol. *32*, 255–264.

Huyer, G., Liu, S., Kelly, J., Moffat, J., Payette, P., Kennedy, B., Tsaprailis, G., Gresser, M.J., and Ramachandran, C. (1997). Mechanism of inhibition of protein-tyrosine phosphatases by vanadate and pervanadate. J. Biol. Chem. *272*, 843–851.

Hwang, J., Lee, J.A., and Pallas, D.C. (2016). Leucine carboxyl methyltransferase 1 (LCMT-1) methylates protein phosphatase 4 (PP4) and protein phosphatase 6 (PP6) and differentially regulates the stable formation of different PP4 holoenzymes. J. Biol. Chem. *291*, 21008–21019.

Inoue, D., Kitaura, J., Matsui, H., Hou, H.A., Chou, W.C., Nagamachi, A., Kawabata, K.C., Togami, K., Nagase, R., Horikawa, S., et al. (2015). SETBP1 mutations drive leukemic transformation in ASXL1-mutated MDS. Leukemia *29*, 847–857.

Jackson, J.B., and Pallas, D.C. (2012). Circumventing cellular control of PP2A by methylation promotes transformation in an Akt-dependent manner. Neoplasia *14*, 585–599.

Kake, S., Tsuji, S., Enjoji, S., Hanasaki, S., Hayase, H., Yabe, R., Tanaka, Y., Nakagawa, T., Liu, H.P., Chang, S.C., et al. (2017). The role of SET/I2PP2A in canine mammary tumors. Sci. Rep. *7*, 4279.

Kaur, A., Denisova, O.V., Qiao, X., Jumppanen, M., Peuhu, E., Ahmed, S.U., Raheem, O., Haapasalo, H., Eriksson, J., Chalmers, A.J., et al. (2016). PP2A inhibitor PME-1 drives kinase inhibitor resistance in glioma cells. Cancer Res. *76*, 7001–7011.

Kawashima, I., and Kirito, K. (2016). Metformin inhibits JAK2V617F activity in MPN cells by activating AMPK and PP2A complexes containing the B56alpha subunit. Exp. Hematol. *44*, 1156–1165.e4.

Kettenbach, A.N., Schweppe, D.K., Faherty, B.K., Pechenick, D., Pletnev, A.A., and Gerber, S.A. (2011). Quantitative phosphoproteomics identifies

substrates and functional modules of Aurora and Polo-like kinase activities in mitotic cells. Sci. Signal. *4*, rs5.

Kim, S.H., Markham, J.A., Weiler, I.J., and Greenough, W.T. (2008). Aberrant early-phase ERK inactivation impedes neuronal function in fragile X syndrome. Proc. Natl. Acad. Sci. U S A *105*, 4429–4434.

Kotecki, M., Reddy, P.S., and Cochran, B.H. (1999). Isolation and characterization of a near-haploid human cell line. Exp. Cell Res. *252*, 273–280.

Liu, X., Huai, J., Endle, H., Schlüter, L., Fan, W., Li, Y., Richers, S., Yurugi, H., Rajalingam, K., Ji, H., et al. (2016). PRG-1 regulates synaptic plasticity via intracellular PP2A/β1-integrin signaling. Dev. Cell *38*, 275–290.

Longin, S., Zwaenepoel, K., Louis, J.V., Dilworth, S., Goris, J., and Janssens, V. (2007). Selection of protein phosphatase 2A regulatory subunits is mediated by the C terminus of the catalytic subunit. J. Biol. Chem. *282*, 26971–26980.

Lucas, C.M., Harris, R.J., Giannoudis, A., Copland, M., Slupsky, J.R., and Clark, R.E. (2011). Cancerous inhibitor of PP2A (CIP2A) at diagnosis of chronic myeloid leukemia is a critical determinant of disease progression. Blood *117*, 6660–6668.

Lucas, C.M., Scott, L.J., Carmell, N., Holcroft, A.K., Hills, R.K., Burnett, A.K., and Clark, R.E. (2018). CIP2A- and SETBP1-mediated PP2A inhibition reveals AKT S473 phosphorylation to be a new biomarker in AML. Blood Adv. *2*, 964–968.

Luo, W., Slebos, R.J., Hill, S., Li, M., Brábek, J., Amanchy, R., Chaerkady, R., Pandey, A., Ham, A.J., and Hanks, S.K. (2008). Global impact of oncogenic Src on a phosphotyrosine proteome. J. Proteome Res. *7*, 3447–3460.

MacLean, B., Tomazela, D.M., Shulman, N., Chambers, M., Finney, G.L., Frewen, B., Kern, R., Tabb, D.L., Liebler, D.C., and MacCoss, M.J. (2010). Skyline: an open source document editor for creating and analyzing targeted proteomics experiments. Bioinformatics *26*, 966–968.

Mair, A., Pedrotti, L., Wurzinger, B., Anrather, D., Simeunovic, A., Weiste, C., Valerio, C., Dietrich, K., Kirchler, T., Nägele, T., et al. (2015). SnRK1-triggered switch of bZIP63 dimerization mediates the low-energy response in plants. eLife *4*, e05828.

Mazhar, S., Leonard, D., Sosa, A., Schlatzer, D., Thomas, D., and Narla, G. (2020). Challenges and Reinterpretation of Antibody-Based Research on Phosphorylation of Tyr307 on PP2Ac. Cell Rep. *30*, this issue, 3164–3170.

Mukhopadhyay, A., Hanold, L.E., Thayele Purayil, H., Gisemba, S.A., Senadheera, S.N., and Aldrich, J.V. (2017). Macrocyclic peptides decrease c-Myc protein levels and reduce prostate cancer cell growth. Cancer Biol. Ther. *18*, 571–583.

Narla, G., Sangodkar, J., and Ryder, C.B. (2018). The impact of phosphatases on proliferative and survival signaling in cancer. Cell. Mol. Life Sci. *75*, 2695–2718.

Neviani, P., Santhanam, R., Trotta, R., Notari, M., Blaser, B.W., Liu, S., Mao, H., Chang, J.S., Galietta, A., Uttam, A., et al. (2005). The tumor suppressor PP2A is functionally inactivated in blast crisis CML through the inhibitory activity of the BCR/ABL-regulated SET protein. Cancer Cell *8*, 355–368.

Nunbhakdi-Craig, V., Schuechner, S., Sontag, J.M., Montgomery, L., Pallas, D.C., Juno, C., Mudrak, I., Ogris, E., and Sontag, E. (2007). Expression of protein phosphatase 2A mutants and silencing of the regulatory B alpha subunit induce a selective loss of acetylated and detyrosinated microtubules. J. Neurochem. *101*, 959–971.

Oaks, J.J., Santhanam, R., Walker, C.J., Roof, S., Harb, J.G., Ferenchak, G., Eisfeld, A.K., Van Brocklyn, J.R., Briesewitz, R., Saddoughi, S.A., et al. (2013). Antagonistic activities of the immunomodulator and PP2A-activating drug FTY720 (Fingolimod, Gilenya) in Jak2-driven hematologic malignancies. Blood *122*, 1923–1934.

Ogris, E., Gibson, D.M., and Pallas, D.C. (1997). Protein phosphatase 2A subunit assembly: the catalytic subunit carboxy terminus is important for binding cellular B subunit but not polyomavirus middle tumor antigen. Oncogene *15*, 911–917.

Ogris, E., Sontag, E., Wadzinski, B., and Narla, G. (2018). Specificity of research antibodies: "trust is good, validation is better". Hum. Pathol. *72*, 199–201.

Pear, W.S., Nolan, G.P., Scott, M.L., and Baltimore, D. (1993). Production of high-titer helper-free retroviruses by transient transfection. Proc. Natl. Acad. Sci. U S A *90*, 8392–8396.

Piazza, R., Valletta, S., Winkelmann, N., Redaelli, S., Spinelli, R., Pirola, A., Antolini, L., Mologni, L., Donadoni, C., Papaemmanuil, E., et al. (2013). Recurrent SETBP1 mutations in atypical chronic myeloid leukemia. Nat. Genet. *45*, 18–24.

Rappsilber, J., Mann, M., and Ishihama, Y. (2007). Protocol for micro-purification, enrichment, pre-fractionation and storage of peptides for proteomics using StageTips. Nat. Protoc. *2*, 1896–1906.

Richard, N.P., Pippa, R., Cleary, M.M., Puri, A., Tibbitts, D., Mahmood, S., Christensen, D.J., Jeng, S., McWeeney, S., Look, A.T., et al. (2016). Combined targeting of SET and tyrosine kinases provides an effective therapeutic approach in human T-cell acute lymphoblastic leukemia. Oncotarget *7*, 84214–84227.

Rincón, R., Cristóbal, I., Zazo, S., Arpí, O., Menéndez, S., Manso, R., Lluch, A., Eroles, P., Rovira, A., Albanell, J., et al. (2015). PP2A inhibition determines poor outcome and doxorubicin resistance in early breast cancer and its activation shows promising therapeutic effects. Oncotarget *6*, 4299–4314.

Roberts, K.G., Smith, A.M., McDougall, F., Carpenter, H., Horan, M., Neviani, P., Powell, J.A., Thomas, D., Guthridge, M.A., Perrotti, D., et al. (2010). Essential requirement for PP2A inhibition by the oncogenic receptor c-KIT suggests PP2A reactivation as a strategy to treat c-KIT+ cancers. Cancer Res. *70*, 5438–5447.

Roncador, G., Engel, P., Maestre, L., Anderson, A.P., Cordell, J.L., Cragg, M.S., Šerbec, V.C., Jones, M., Lisnic, V.J., Kremer, L., et al. (2016). The European antibody network's practical guide to finding and validating suitable antibodies for research. MAbs *8*, 27–36.

Schmitz, M.H., Held, M., Janssens, V., Hutchins, J.R., Hudecz, O., Ivanova, E., Goris, J., Trinkle-Mulcahy, L., Lamond, A.I., Poser, I., et al. (2010). Live-cell imaging RNAi screen identifies PP2A-B55alpha and importin-beta1 as key mitotic exit regulators in human cells. Nat. Cell Biol. *12*, 886–893.

Sents, W., Ivanova, E., Lambrecht, C., Haesen, D., and Janssens, V. (2013). The biogenesis of active protein phosphatase 2A holoenzymes: a tightly regulated process creating phosphatase specificity. FEBS J. *280*, 644–661.

Sontag, J.M., and Sontag, E. (2014). Protein phosphatase 2A dysfunction in Alzheimer's disease. Front. Mol. Neurosci. *7*, 16.

Stanevich, V., Jiang, L., Satyshur, K.A., Li, Y., Jeffrey, P.D., Li, Z., Menden, P., Semmelhack, M.F., and Xing, Y. (2011). The structural basis for tight control of PP2A methylation and function by LCMT-1. Mol. Cell *41*, 331–342.

Sun, Y., Zheng, Q., Sun, Y.T., Huang, P., Guo, Z.L., and Xu, L.H. (2014). Microcystin-LR induces protein phosphatase 2A alteration in a human liver cell line. Environ. Toxicol. *29*, 1236–1244.

Taussig, M.J., Fonseca, C., and Trimmer, J.S. (2018). Antibody validation: a view from the mountains. N. Biotechnol. *45*, 1–8.

Tolstykh, T., Lee, J., Vafai, S., and Stock, J.B. (2000). Carboxyl methylation regulates phosphoprotein phosphatase 2A by controlling the association of regulatory B subunits. EMBO J. *19*, 5682–5691.

Velmurugan, B.K., Lee, C.H., Chiang, S.L., Hua, C.H., Chen, M.C., Lin, S.H., Yeh, K.T., and Ko, Y.C. (2018). PP2A deactivation is a common event in oral cancer and reactivation by FTY720 shows promising therapeutic potential. J. Cell. Physiol. *233*, 1300–1311.

Virshup, D.M., and Shenolikar, S. (2009). From promiscuity to precision: protein phosphatases get a makeover. Mol. Cell *33*, 537–545.

Vizcaíno, J.A., Côté, R.G., Csordas, A., Dianes, J.A., Fabregat, A., Foster, J.M., Griss, J., Alpi, E., Birim, M., Contell, J., et al. (2013). The PRoteomics IDEntifications (PRIDE) database and associated tools: status in 2013. Nucleic Acids Res. *41*, D1063–D1069.

Wandzioch, E., Pusey, M., Werda, A., Bail, S., Bhaskar, A., Nestor, M., Yang, J.J., and Rice, L.M. (2014). PME-1 modulates protein phosphatase 2A activity to promote the malignant phenotype of endometrial cancer cells. Cancer Res. *74*, 4295–4305.

Wang, X., Chen, Y., Zuo, X., Ding, N., Zeng, H., Zou, X., and Han, X. (2013). Microcystin (-LR) induced testicular cell apoptosis via up-regulating apoptosis-related genes in vivo. Food Chem. Toxicol. *60*, 309–317.

Wang, H., Liu, J., Lin, S., Wang, B., Xing, M., Guo, Z., and Xu, L. (2014). MCLR-induced PP2A inhibition and subsequent Rac1 inactivation and hyperphosphorylation of cytoskeleton-associated proteins are involved in cytoskeleton rearrangement in SMMC-7721 human liver cancer cell line. Chemosphere *112*, 141–153.

Wang, B., Liu, J., Huang, P., Xu, K., Wang, H., Wang, X., Guo, Z., and Xu, L. (2017). Protein phosphatase 2A inhibition and subsequent cytoskeleton reorganization contributes to cell migration caused by microcystin-LR in human laryngeal epithelial cells (Hep-2). Environ. Toxicol. *32*, 890–903.

Weller, M.G. (2018). Ten basic rules of antibody validation. Anal. Chem. Insights *13*, 1177390118757462.

Xu, C., Wang, X., Zhu, Y., Dong, X., Liu, C., Zhang, H., Liu, L., Huang, S., and Chen, L. (2016). Rapamycin ameliorates cadmium-induced activation of MAPK pathway and neuronal apoptosis by preventing mitochondrial ROS inactivation of PP2A. Neuropharmacology *105*, 270–284.

Yabe, R., Tsuji, S., Mochida, S., Ikehara, T., Usui, T., Ohama, T., and Sato, K. (2018). A stable association with PME-1 may be dispensable for PP2A demethylation - implications for the detection of PP2A methylation and immunoprecipitation. FEBS Open Bio *8*, 1486–1496.

Yu, X.X., Du, X., Moreno, C.S., Green, R.E., Ogris, E., Feng, Q., Chou, L., McQuoid, M.J., and Pallas, D.C. (2001). Methylation of the protein phosphatase 2A catalytic subunit is essential for association of Balpha regulatory subunit but not SG2NA, striatin, or polyomavirus middle tumor antigen. Mol. Biol. Cell *12*, 185–199.

STAR★METHODS

KEY RESOURCES TABLE

REAGENT or RESOURCE	SOURCE	IDENTIFIER
Antibodies		
PP2A catalytic subunit: C-sub Nterm (H8), mouse monoclonal	Ogris Lab stock (Frohner et al., 2020)	N/A
PP2A catalytic subunit: Sat20, rabbit polyclonal	Ogris Lab stock (Fellner et al., 2003)	N/A
PP2A catalytic subunit: E155, rabbit monoclonal	Abcam	Cat# ab32104, lot# GR96171-13; RRID:AB_777385
PP2A catalytic subunit pTyr307: SCBT goat, goat polyclonal	Santa Cruz Biotechnology	Cat# sc-12615, lots A2413 and L0413, discontinued; RRID:AB_670858
PP2A catalytic subunit pTyr307: SCBT rabbit, rabbit polyclonal	Santa Cruz Biotechnology	Cat# sc-12615-R, lot F2413, discontinued; RRID:AB_670859
PP2A catalytic subunit pTyr307: SCBT F8, mouse monoclonal	Santa Cruz Biotechnology	Cat# sc-271903, lot C1617; RRID:AB_10611810
PP2A catalytic subunit pTyr307: R&D, rabbit polyclonal	R&D Systems, # AF3989 lot YZW04166111	Cat# AF3989, lot YZW0416111; RRID:AB_2169636
PP2A catalytic subunit pTyr307: 4B10, mouse monoclonal	Ogris Lab stock	N/A
PP2A catalytic subunit pTyr307: Sigma, rabbit polyclonal	SigmaAldrich/Merck	Cat#SAB4503975, lot 110555
PP2A catalytic subunit pTyr307: Thermo, rabbit polyclonal	Thermo Fischer	Cat# PA5-36874, lot UC2737255; RRID:AB_2553794
General P-tyr: pTyr 1000, P-Tyr-1000 MultiMab Rabbit mAb mix,	Cell Signaling Technology	Cat# 8954, lot 8; RRID:AB_2687925
General P-tyr: pTyr 100, mouse monoclonal,	Cell Signaling Technology	Cat#9411, lot 27; RRID:AB_331228
General P-tyr: 4G10, mouse monoclonal	kindly provided by Dr. John Alberta and Dr. Thomas Roberts, DFCI, Harvard Medical School, Boston	N/A
non me-PP2A C, 1D7, mouse monoclonal	Ogris Lab stock, (Frohner et al., 2020)	N/A
me-PP2A C, 7C10, mouse monoclonal	Ogris Lab stock, (Frohner et al., 2020)	N/A
HA, clone 16B12, mouse monoclonal	Covance	Cat# MMS-101R, lot B211583; RRID:AB_291262
HA 12CA5, mouse monoclonal	Ogris Lab stock, (Green et al., 1982)	N/A
myc 4A6, mouse monoclonal	Ogris Lab stock, (Hombauer et al., 2007)	N/A
pSrc416, clone D49G4, rabbit monoclonal	Cell Signaling Technology	Cat# 6943, lot 4; RRID:AB_10013641
Lcmt-1, rabbit polyclonal	Ogris Lab stock (Frohner et al., 2020)	N/A
pan-actin, clone 2A3-6A5-G2, mouse monoclonal	Ogris Lab stock (Frohner et al., 2020)	N/A
GAPDH, clone 6C5, mouse monoclonal	Abcam	Cat# ab8245, lot GR137268-14; RRID:AB_2107448
SET/TAF-I, rabbit monoclonal,	Abcam	Cat# ab176567, lotGR137929-S
Anti-mouse HRP, goat polyclonal, IgG, Fcγ fragment specific	Jackson ImmunoResearch	Cat# 115-035-008 lot 124594; RRID:AB_2313585
Anti-rabbit HRP, goat polyclonal,IgG, Fc fragment specific	Jackson ImmunoResearch	Cat# 111-035-008, lot 129411; RRID:AB_2337937
Anti-goat HRP, rabbit polyclonal, IgG, Fc fragment specific	Jackson ImmunoResearch	Cat# 305-035-008, lot 125727; RRID:AB_2339402
Biotin anti-mouse CD11b clone MEL1/70, rat monoclonal	BioLegend	Cat# 101204; RRID:AB_312787
Biotin anti-mouse CD11c, clone N418,	BioLegend	Cat# 117304; RRID:AB_313773

(*Continued on next page*)

Continued

REAGENT or RESOURCE	SOURCE	IDENTIFIER
Biotin anti-mouse B220 clone RA3-6B2, rat monoclonal	BioLegend	Cat# 103204; RRID:AB_312989
Biotin anti-mouse Gr1 clone RB6-8C5, rat monoclonal	BioLegend	Cat# 108404; RRID:AB_312989
Biotin anti-mouse NK1.1, clone PK136, mouse monoclonal	BioLegend	Cat# 108704; RRID:AB_313391
Biotin anti-mouse Ter-119, clone Ter-119, rat monoclonal	BioLegend	Cat#116204; RRID:AB_313705
Biotin anti-mouse CD8α, clone 53-6.7, rat monoclonal	BioLegend	Cat# 100704; RRID:AB_312743
Biotin anti-mouse CD25, clone PC61, rat monoclonal	BioLegend	Cat# 102004; RRID:AB_312853
Biotin anti-mouse CD44, clone IM7, rat monoclonal	BioLegend	Cat#103004; RRID:AB_312955
Anti-mouse CD3ε, clone 145-2C11, Armenian hamster monoclonal	BD Biosciences	Cat#553057; RRID:AB_394590
Anti-mouse CD28, clone 37.51, Syrian hamster monoclonal	BD Biosciences	Cat#553294; RRID:AB_394763
PE anti-mouse CD19, clone 1D3, rat monoclonal	BD Biosciences	Cat#557399; RRID:AB_396682
APC/Cy7 anti-mouse TCRβ, clone H57-597, Armenian Hamster IgG	BioLegend	Cat#109220; RRID:AB_893624
PE/Cy7 anti-mouse CD4, clone RM4-5, rat monoclonal	BioLegend	Cat#100527; RRID:AB_312728
APC, anti-mouse CD8α, clone 53-6.7, rat monoclonal	Thermo Scientific	Cat#17-0081-83; RRID:AB_469336
PE, anti-mouse CD62L, clone MEL-14, rat monoclonal	BD Biosciences	Cat#553151; RRID:AB_394666
Brilliant Violet 421 anti-mouse/human CD44, clone IM7, rat monoclonal	BioLegend	Cat#103039; RRID:AB_10895752
Chemicals, Peptides, and Recombinant Proteins		
Dulbecco's Modified Eagle's Medium (DMEM),	Sigma	# D5671
Iscove's Modified Dulbecco's Medium (IMDM),	Thermo Fisher Scientific, Life Technologies	#12440053
Turbofectin 8.0	Origene	#TF81001
Abl127	Merck Sigma-Aldrich	SML0294
Okadaic acid (OA),	Tocris	# 1136
cOmplete	Roche	#11836145001
BSA-coated protein A-Sepharose beads CL-4B	GE-Healthcare	#17-0780-01, lot 10254134
HA synthetic peptides	EMC Microcollections	N/A
PP2Ac synthetic peptides	piCHEM	N/A
Deposited Data		
MS proteomics data	this study	ProteomeXchange Consortium, PXD014879
Western Blot Dataset	this study	https://data.mendeley.com/datasets/9fp33f2xc8/draft?a=4fbadc7b-bc47-43b4-a888-1e1bf51acd41
List of publications using commercial $PP2A_C$ $pTyr^{307}$ antibodies	this study	https://data.mendeley.com/datasets/8pn49xwxbk/draft?a=f36e50a7-3885-41ce-9797-8c9cec5c77d6
Experimental Models: Cell Lines		
HAP1 wild type	Horizon Discovery	# C631
HAP1, *Lcmt1*$^{-}$	Horizon Discovery	# HZGHC004373c001
HEK293T	Provided by Thomas Leonard, Max Perutz Labs, ATCC	CRL-3216
NIH 3T3	Provided by Wilhelm Krek, ETH Zürich, ATCC	CRL-1658
BOSC-23	(Pear et al., 1993)	N/A
Neuro-2a (N2a)	ATCC	CCL-131

(*Continued on next page*)

Continued

REAGENT or RESOURCE	SOURCE	IDENTIFIER
Cos-7	ATCC	CRL-1651
Recombinant DNA and Plasmids		
pBabe puro	(Fellner et al., 2003)	N/A
pBabe puro HA-PP2AC	(Fellner et al., 2003)	N/A
pcDNA3 puro	(Frohner et al., 2020)	N/A
pcDNA3 puro HA PP2Ac	(Frohner et al., 2020)	N/A
pcDNA3 puro myc PP2AC	this study	N/A
pcDNA3 puro myc PP2AC Y307F	this study	N/A
pSrc$^{(CA)}$	(Luo et al., 2008)	N/A
Software and Algorithms		
ImageJ	NIH	RRID: SCR_003070
Excel	Microsoft Excel,	RRID:SCR_016137
Real Statistics Resource Pack software (Release 6.2)	Charles Zaiontz	www.real-statistics.com

LEAD CONTACT AND MATERIALS AVAILABILITY

Further information and requests for resources and reagents should be directed to the Lead Contact, Egon Ogris (egon.ogris@meduniwien.ac.at) and will be fulfilled upon completion of a Materials Transfer Agreement.

EXPERIMENTAL MODEL AND SUBJECT DETAILS

Cell Lines

HAP1 wild-type and Leucine carboxyl methyltransferase 1 knockout (*Lcmt-1*$^{-}$) cells (Horizon Discovery, # C631 and # HZGHC004373c001) were grown in Iscove's Modified Dulbecco's Medium (IMDM, Thermo Fisher Scientific, Life Technologies #12440-053, lot 2120381) supplemented with 10% (v/v) Fetal Calf Serum (FCS) (Sigma # F7524, lot 104M3333), GlutaMAX^{TM} (Thermo Fisher Scientific, Life Technologies #35050-38, lot 1895829), and penicillin-streptomycin Solution (Sigma, #P4333, lot 125M4781V) at 5% CO_2 and 37°C. HEK293T, NIH 3T3, and BOSC-23 (Pear et al., 1993) cells were grown in Dulbecco's Modified Eagle's Medium (DMEM, Sigma # D5671, lot RNBG4527) supplemented with 10% (v/v) FBS, GlutaMAX^{TM} and Penicillin-Streptomycin Solution at 7.5% CO_2 and 37°C

Neuro-2a (N2a) and Cos-7 (American Type Culture Collection) cell lines were maintained in DMEM (Life Technologies Australia Pty Ltd, Australia) containing 25 mM HEPES, pH 7.4, 10% FBS (Bovogen, France), and 10 μg/ml gentamycin (Life Technologies Australia Pty Ltd, Australia) at 5% CO_2 and 37°C.

Animals

The maintenance of mice and experimental procedures have been conducted according to the Austrian Animal Experiments Act and have been approved by the Austrian Federal Ministry of Science and Research (GZ 66.009/74-Pr/4/98) and the animal experiments ethics committee of the Medical University of Vienna. Mice were regularly monitored with respect to general health. Female Balb/C mice 12 weeks of age were used for antigen immunization.

METHOD DETAILS

Mammalian Tissue Culture

NIH 3T3 cells were infected using viral supernatant produced in BOSC-23 cells. For detection of pTyr PP2A$_C$ subunit, exponentially growing NIH 3T3 cells were counted using an automated cell counter (Luna^{TM} Biozyme) and 6 × 10^6 cells were plated per p150 dish. After 6 hours, cells were washed with DMEM and starved with DMEM containing 0.5% FBS for 17 hours. The samples were processed as described below in the section Immunoprecipitation and Western Blot. For transient transfection and HEK293T cells, cells were plated on p60 dishes the day before transfection. 5μg of pcDNA vector constructs were cotransfected with 2μg of the Src$^{(CA)}$ construct using Turbofectin (Origene, #TF81001, lot 91033816) as transfection reagent. 24 hours after the transfection the cells were expanded to a p100 plate and cell lysates were prepared 43 hours after transfection as described below.

Neuro-2a and Cos-7 cells were transiently transfected with the indicated plasmids using Metafectene Pro reagent following the manufacturer's instructions (Biontex laboratories, Germany). Cells mock-transfected with empty vectors (EV) were used as ''controls'' and behaved like non-transfected cells in our experiments. Unless otherwise indicated, experiments were performed

using ~80% confluent cells cultured in regular cell culture medium. When indicated, cells were serum-starved overnight in medium containing 0.1% FBS and treated for 15 min with 100 μM pervanadate

Plasmids

pcDNA3 puro, pcDNA3 puro HA PP2AC wt (Frohner et al., 2020), pcDNA3 puro myc $PP2A_C$ wt and pcDNA3 puro myc $PP2A_C$ Y307F (this study), pBabepuro, pBabepuro HA-$PP2A_C$ (Fellner et al., 2003), $pSrc^{(CA)}$ (Luo et al., 2008).

Antibodies

PP2A catalytic subunit antibodies

Mouse monoclonal antibody (mAb), clone H8, was raised against 1-144 aa of human PP2A catalytic subunit, α isoform (Frohner et al., 2020). Rabbit polyclonal antibody (RpAb), Sat20, was raised against 288-303aa of human PP2A catalytic subunit α isoform (Fellner et al., 2003). Rabbit monoclonal antibody (rmAb), E155, was raised against a synthetic peptide (the exact sequence is not disclosed by Abcam) corresponding to human PP2A catalytic subunit, α and β isoform (Abcam, since 2016 sold as PP2A alpha + beta antibody; ab32104, lot GR96171-13, before 2016 it was sold as Phospho-PP2A (Tyr^{307}) rmAb). This antibody was originally generated by Epitomics, Inc., Burlingame, California, U.S. The Epitomics product data sheet (# 1155-1) indicated that the antibody was raised against a synthetic phosphopeptide corresponding to residues encompassing $pTyr^{307}$ of human $PP2A_C$. For further information about antibody E155 see: Specificity of research antibodies: ''trust is good, validation is better'' (Ogris et al., 2018).

PP2A catalytic subunit $pTyr^{307}$ antibodies

Goat polyclonal antibodies (gpAb), SCBT goat, was raised against a short amino acid sequence containing phosphorylated Tyr^{307} of mouse PP2A catalytic subunit, α isoform (exact immunogen sequence not disclosed, Santa Cruz Biotechnology # sc-12615, lots A2413 and L0413, discontinued), and rpAB, SCBT rabbit, was raised against a short amino acid sequence containing phosphorylated Tyr^{307} of mouse PP2A catalytic subunit, α isoform (exact immunogen sequence not disclosed, Santa Cruz Biotechnology, sc-12615-R, lot F2413, discontinued). mAb, SCBT mouse, was raised against a short amino acid sequence containing phosphorylated Tyr^{307} of mouse PP2A catalytic subunit, α isoform (exact immunogen sequence not disclosed, Santa Cruz Biotechnology # sc-271903, lot C1617, clone F-8). RpAb, R&D, was raised against a phosphopeptide containing human PP2A Tyr^{307} site (exact immunogen sequence not disclosed, R&D Systems, # AF3989 lot YZW0416111). mAb, 4B10, was raised against a 302-309aa peptide of human PP2A catalytic subunit phosphorylated at Tyr^{307} (this study, Millipore # 05-547, discontinued, also available from BioLegend/Covance, BioTechne/Novus and SCBT; Ogris lab stock was used in all experiments), RpAb, Sigma was raised against a phosphopeptide containing human $PP2A_C$ Tyr^{307} site (exact immunogen sequence not disclosed, SigmaAldrich, #SAB4503975 lot 110555), RpAb, Thermo Fisher was raised against a synthetic phosphopeptide derived from human $PP2A_C$ α isoform around the phosphorylation site of Tyrosine 307 (Thermo Fisher, # PA5-36874, lot UC2737255).

P-Tyr specific antibodies

RmAb, pY1000, (Cell signaling P-Tyr-1000 MultiMab Rabbit mAb mix # 8954, lot 8), mAb pY100, raised against phospho-tyrosine containing peptides (Cell signaling p-Tyr-100 #9411, lot 27), mAb 4G10 (kindly provided by Dr. John Alberta and Dr. Thomas Roberts, DFCI, Harvard Medical School, Boston),

PP2A antibodies against C terminus

mAb, non me-C sub 1D7, was raised against 304-309aa of human PP2A catalytic subunit (Ogris lab stock), mAb, me-C sub 7C10, was raised against 304-309aa of human PP2A catalytic subunit methylated at leucine-309 (Ogris lab stock).

Other Antibodies

mAb, HA 16B12, was raised against the twelve amino acid peptide CYPYDVPDYASL (Covance #MMS-101R, lot B211583). mAb, HA 12CA5, was raised against 76-111aa from the human influenza virus hemagglutinin protein (Green et al., 1982) (Ogris lab stock), rbAb, Lcmt-1, raised against full length human leucin carboxy methyl transferase-1 (Ogris lab stock, non-purified (Frohner et al., 2020), mAb, pan-actin 2A3-6A5-G2, was raised against 358-374aa of the human beta-actin C terminus (Ogris lab stock) (Frohner et al., 2020), mAb, GAPDH Clone 6C5 (Abcam, #ab8245, lot GR137268-14). RmAb SET/TAF-I (Abcam, #ab176567, lotGR137929-S), mAb, myc 4A6 (Ogris lab stock, also available at Millipore #05-724, Hombauer et al., 2007), rmABb, pSrc p416, clone D49G4 (Cell signaling #6943)

Secondary peroxidase conjugated antibodies

Anti-mouse, anti-rabbit or anti-goat antibody (Jackson ImmunoResearch, goat anti mouse #115-035-008 lot 124594, goat anti rabbit: #111-035-008, lot 129411; rabbit anti goat: #305-035-008, lot 125727)

Cell Lysis, Alkaline and Phosphatase Treatment

Cells were lysed in IP Lyse buffer (1% Nonidet P-40; 10% (vol/vol) glycerol; 135 mM NaCl; 20 mM Tris, pH 8.0; 1mM PMSF; 0.03 units/ml aprotinin (Sigma), 1x Complete (Roche), 1mM orthovanadate, 10mM beta-glycerophosphate, 1μM Okadaic acid, 2μM Abl127) for 20 min with rocking at 4°C. Lysates were scraped and cleared at 13 000 g and normalized for total protein concentration. For calf intestinal phosphatase (CIP, NEB) treatment cells were lysed in IP Lyse buffer without phosphatase inhibitors and EDTA. Lysates were incubated with 0.5 Units of CIP per μg lysate for 1 hour at room temperature. Control lysate was mock incubated for 1 hour at room temperature without phosphatase treatment. For alkaline treatment, 100μl of lysate (untreated or CIP treated) was mixed with NaOH to a final concentration of 0.2M and incubated for 10 min at RT. The reaction was neutralized by adding HCl to a final concentration

of 0.2M and diluted to 200 μl with IP Lyse. The control reaction was treated with preneutralization solution (0.2M NaOH and 0.2M HCl) and diluted to 200μl with IP Lyse. The samples were boiled with protein sample buffer (Laemmli) for immunoblot analysis.

Total N2a and Cos-7 cell homogenates were prepared in Buffer 1 [25 mM Tris, pH 7.4, 150 mM NaCl, 1 mM dithiothreitol (DTT), 0.5 μM okadaic acid (OA, Merck Millipore), 5 mM PMSF (Sigma), 1% NP-40 (Sigma), Sigma Protease Inhibitor Cocktail™, and Sigma Phosphatase Inhibitor Cocktail™], and cleared by centrifugation at 4°C for 5 min at 13,000 x *g*. When indicated, a duplicate aliquot of cell lysate was treated for 1h at 30°C with alkaline phosphatase (AP; 1 unit/ μg protein; Roche) to induce global protein dephosphorylation, prior to addition of the gel loading buffer. Total cell lysates (~50 μg) were resolved by SDS-PAGE on NU-PAGE 4%–12% Bis-Tris gels (Thermo Fisher Scientific). Prestained Protein Standards (BIO-RAD) were used as molecular weight standards. Western blotting was performed using the indicated primary antibodies followed by Infrared IRDye®-labeled secondary antibodies and visualized using the Odyssey™ Infrared imaging system (LI-COR Biosciences).

Immunoprecipitation and Western Blot

Whole cell protein lysates of cell lines were incubated either with 12CA5 antibody crosslinked to BSA-coated protein A-Sepharose beads CL-4B (GE-Healthcare #17-0780-01, lot 10254134). The immune complexes were washed once with IP-Lyse and 3 x with Tris-buffered saline. The beads were boiled for 5min at 95°C in protein sample buffer (Laemmli) for immunoblot analysis. Samples were separated by SDS-polyacrylamide gels and were blotted on nitrocellulose membrane (GE Healthcare, 0.2μm). Membranes were stained with PonceauS, blocked with 3% non-fat dry milk (NFDM) in TBS-Tween-20 (0.05%) for phosphotyrosine antibodies and 3% non-fat dry milk in PBS-Tween-20 (0.05%) for all other antibodies. To remove phosphate groups on proteins the membranes were treated with calf intestine alkaline phosphatase (CIP, New England Biolabs #M0290, 66U/ml) at 30°C for 30min. The membranes were blocked with 3% NFDM in TBS-Tween-20 for 1 hour at RT and incubated with primary antibody at the following dilutions (HA 16B12 1:20000, Abcam E155 1:5000, SCBT antibodies all 1:500, R&D 1:1000, Sigma and Thermo Fisher 1:2000, $PP2A_C$ N-terminal H8 1:100, me-C sub 7C10 1:100, non me-C sub 1D7 1:200, pan-actin 1:1000, Sat20 1:10000, Lcmt-1 poly 1:10000, pY-1000 1:5000, pY-100 1:1000, myc 4A6 1:2000, src^{416} 1:2000, pTyr 4G10 1:5000, SET/TAF-I 1:10000) in 0.5% NFDM/TBS-Tween-20 o/n at 4°C. Incubation with secondary peroxidase conjugated anti-mouse (1:10000), anti-rabbit (1:10000) or anti-goat antibodies (1:5000 diluted) was performed for 1 hour at RT, followed by incubation with western blotting detection reagents (GE Healthcare or Biorad) as suggested by the manufacturer. For mass spectrometry analysis of $PP2A_C$ subunit modifications, immunoprecipitations were separated by SDS-PAGE, the proteins in the gel were stained with Instant Blue (Expedeon #ISB1L), and the $PP2A_C$ subunit band was cut out of the gel and treated for mass spectrometry analysis as described below.

Purification and Activation of Naive $CD4^+$ T cells

Cells were isolated from spleen, axillary, brachial, and inguinal lymph nodes (LN) of C57BL/6 mice, then pooled and incubated with a cocktail of biotinylated antibodies (anti-mouse CD11b [MEL1/70, BioLegend #101204], anti-mouse CD11c [N418, Biolegend #117304], anti-mouse B220 [RA3-6B2, BioLegend # 103204], anti-mouse Gr1 [RB6-8C5, BioLegend #108404], anti-mouse NK1.1 [PK136, BioLegend #108704], anti-mouse Ter-119 [Ter-119, BioLegend #116204], anti-mouse CD8α [53-6.7, BioLegend #100704], anti-mouse CD25 [PC61, BioLegend #102004], anti-mouse CD44 [IM7, BioLegend #103004] in PBS/2% FBS). $CD4^+$ T cells were enriched by negative depletion using magnetic streptavidin beads (MagniSort SAV Negative Selection beads, Thermo Scientific #MSNB-6002-74) according to the manufacturer's instructions. MACS-sorted naive $CD4^+$ T cells were stimulated for 24 hours with plate-bound anti-CD3ε (1 μg/ml; BD Biosciences #553057) and anti-CD28 (3 μg/ml; BD Biosciences #553294) on 48-well plates (1×10^6 cells/well) in 1 mL T cell medium/well (RPMI-1640 supplemented with 10% FCS [Biowest]). Cells were harvested and cell pellets were frozen in liquid nitrogen, a cell aliquot was extracellular stained (Viability Dye eFluor® 506 [Thermo Scientific #65-0866-14], CD19 [1D3, BD Biosciences #557399], TCRβ (H57-597, BioLegend #109220), CD4 [RM4-5, BioLegend #100527], CD8α (53-6.7, Thermo Scientific #17-0081-83), CD62L (MEL-14, BD Biosciences #553151) and CD44 [IM7, BioLegend #103039]) for flow cytometry analysis.

Enzyme-Linked Immunosorbent Assay

ELISA 96 well plates (Thermo Scientific, Medisorp) were coated with 50μl peptides (2μg/ml in TBS) at 4°C over-night. The plate was blocked with 2% BSA in TBS for 1 hour at RT and incubated with primary antibodies (Abcam E155, SCBT mouse rabbit and goat ((lot A2413), as well as R&D diluted to 1μg/ml, Sigma $pTyr^{307}$ 1:5000, 4B10 1:200, Me C sub 1:100, pY100 100ng/ml) in TBS for 1h at room temperature. Incubation with secondary peroxidase conjugated anti-mouse (1:10000), anti-rabbit (1:10000) or anti-goat (1:5000 in TBS) was performed for 1hour at RT followed by detection with TMB (3′,5′,5′,5′-tetramethylbenzidine; Sigma, Cat T2885) and H_2O_2 in a sodium acetate buffer pH 6.0. The reaction was stopped by the addition of 1N H_2SO_4 and the absorbance was measured at 450nm, for background correction the absorption of 560nm was subtracted.

Peptides were purchased from piCHEM and EMC respectively.

Peptide sequences:

unmod: Ac-His-Val-Thr-Arg-Arg-Thr-Pro-Asp-Tyr-Phe-Leu-OH
$meLeu^{309}$: Ac-His-Val-Thr-Arg-Arg-Thr-Pro-Asp-Tyr-Phe-Leu-OMe
$pThr^{304}$ – Leu^{309}: Ac-His-Val-Thr-Arg-Arg-pThr-Pro-Asp-Tyr-Phe-Leu-OH

pThr^{304} – meLeu^{309}: Ac-His-Val-Thr-Arg-Arg-pThr-Pro-Asp-Tyr-Phe-Leu-OMe
pTyr^{307} - Leu^{309}: Ac-His-Val-Thr-Arg-Arg-Thr-Pro-Asp-pTyr-Phe-Leu-OH
pTyr^{307} - meLeu^{309}: Ac-His-Val-Thr-Arg-Arg-Thr-Pro-Asp-pTyr-Phe-Leu-OMe
HA unmod: Met-Tyr-Pro-Tyr-Asp-Val-Pro-Asp-Tyr-Ala-Leu-Val-NH_2
HA pTyr^{2}: Met-pTyr-Pro-Tyr-Asp-Val-Pro-Asp-Tyr-Ala-Leu-Val-NH_2
HA pTyr^{4}: Met-Tyr-Pro-pTyr-Asp-Val-Pro-Asp-Tyr-Ala-Leu-Val-NH_2
HA pTyr^{9}: Met-Tyr-Pro-Tyr-Asp-Val-Pro-Asp-pTyr–Ala-Leu-Val-NH_2
Liquid chromatography–Mass spectrometry (LC-MS)

The gel samples were processed as described in detail in Mair et al. (2015). Briefly gel pieces were cut and washed in ammonium-bicarbonate buffer. Disulfide bridges were reduced with dithiothreitol (DTT) and free thiols alkylated with iodoactemide (IAM). After digestion peptides were extracted from the gel by sonication and desalted on custom-made C18 stagetips (Rappsilber et al., 2007).

Peptide samples were separated on an Ultimate 3000 RSLC nano-flow chromatography system (Thermo Fisher Scientific), using a pre-column for sample loading (PepMapAcclaim C18, 2 cm × 0.1 mm, 5 μm, Dionex-Thermo-Fisher) and a C18 analytical column (PepMapAcclaim C18, 50 cm × 0.75 mm, 2 μm, Dionex-Thermo-Fisher), applying a linear gradient from 2 to 35% solvent B (80% acetonitrile, 0.1% formic acid; solvent A 0.1% formic acid) at a flow rate of 230 nl/min over 60 minutes. Eluting peptides were analyzed on a Q Exactive HF Orbitrap mass spectrometer, equipped with a Proxeon nanospray source (all Thermo Fisher Scientific). For the data-dependent mode survey scans were obtained in a mass range of 380–1,500 m/z with lock mass on, at a resolution of 60.000 at 200 m/z and an AGC target value of 3E6. The 10 most intense ions were selected with an isolation width of 2 Da, fragmented in the HCD cell at 27% collision energy and the spectra recorded at a target value of 1E5 and a resolution of 17500. Peptides with a charge of +1 were excluded from fragmentation, the peptide match and exclude isotope features were enabled and selected precursors were dynamically excluded from repeated sampling for 20 s. The same method was used when repeating the experiment with an inclusion list of the peptides of interest.

Raw data were processed using the MaxQuant software package 1.6.0.16 (https://www.maxquant.org/) (Cox and Mann, 2008) searching against the sequences of the PPP2ca construct, the sequences of all the mouse proteins that were identified in the gel bands with at least two unique and razor peptides, and a custom database of common contaminants. The search was performed with full enzyme specificity and a maximum of two missed cleavages. Carbamidomethylation of cysteine residues was set as fixed, oxidation of methionine, phosphorylation of STY, N-terminal protein acetylation and C-terminal protein methylation as variable modifications—all other parameters were set to default. Results were filtered at protein and peptide level for a false discovery rate of 1% and spectra assigned to phosphorylated peptides were validated manually.

For the targeted approach a list of precursors was generated based on the peptides of interest with and without modification and included in a top-5/PRM hybrid method with the following parameters: the resolution for the full scan was set to 60000 (at m/z 200), the AGC target to 3 × 106, maximum fill time to 60 ms. Resolution for the top 5 MS2 scans was set to 30000, the AGC target to 1 × 105, maximum fill time to 100 ms. PRM was scheduled based on the retention time observed in previous experiments. PRM settings were 30000 resolution (at m/z 200), AGC target 2 × 105. The maximum fill time was 250 ms, the isolation window was set to 0.7 Da and isolation offset to 0.2 Da. Normalized collision energy of 28 was applied for fragmentation.

Data analysis, manual validation of all peptides and their transitions (based on retention time, relative ion intensities, and mass accuracy), and relative quantification was performed in Skyline (MacLean et al., 2010). In parallel a database search was performed with MaxQuant with the described parameters.

Samples included are listed in Table S3.

QUANTIFICATION AND STATISTICAL ANALYSIS

X-ray films of 1-2 exposures were scanned using a CanoScan LiDE220 scanner (Canon) and ImageJ was used for quantification of western blot signals. Statistical tests were performed in Excel using the Real Statistics Add-In. At least three independent experiments were performed and data were presented as mean ± standard deviation. We assumed a normal distribution of the samples and multiple comparisons were assessed using one-way analysis of variance (ANOVA), followed by a Tukey HSD post hoc test. A p value of < 0.05 was considered statistically significant.

DATA AND CODE AVAILABILITY

The mass spectrometry proteomics data have been deposited to the ProteomeXchange Consortium (http://proteomecentral.proteomexchange.org) via the PRIDE partner repository (Vizcaíno et al., 2013) with the dataset identifier PXD014879.

Original Western Blot data are deposited on Mendeley https://data.mendeley.com/datasets/9fp33f2xc8/draft?a=4fbadc7b-bc47-43b4-a888-1e1bf51acd41.

The list of publications using commercial PP2A$_C$ pTyr^{307} antibodies can be found on Mendeley https://data.mendeley.com/datasets/8pn49xwxbk/draft?a=f36e50a7-3885-41ce-9797-8c9cec5c77d6